Applied Geochemistry 102 (2019) 1–25

Contents lists available at ScienceDirect

Applied Geochemistry

journal homepage: www.elsevier.com/locate/apgeochem

Invited Review

Vanadium geochemistry in the biogeosphere –speciation, solid-solution interactions, and ecotoxicity

Jon Petter Gustafsson[a,b,*]

[a] Department of Soil and Environment, Swedish University of Agricultural Sciences, Box 7014, 750 07, Uppsala, Sweden
[b] KTH Royal Institute of Technology, Department of Sustainable Development, Environmental Science and Engineering, Teknikringen 10B, 100 44, Stockholm, Sweden

ARTICLE INFO

Editorial handling by Prof. M. Kersten

Keywords:
Vanadate
Vanadyl
Water
Soil
Sediment
Bioavailability

ABSTRACT

Vanadium is a metal that receives increasing attention due to its possible toxicity and its increased use in society, i.e. in high-grade steel and in vanadium redox-flow batteries. Already today, the global biogeochemical cycle of vanadium is heavily impacted by human activities, and these impacts will probably increase. The total V concentration in the upper part of the Earth's crust, and in soils, is near 100 mg V kg^{-1}. Usually, the dissolved V concentration is low. In seawater the mean dissolved V concentration is 1.8 µg L^{-1}, and in freshwaters the concentration is commonly below 1 µg L^{-1} although in areas with volcanic and sedimentary rocks it may be much higher, i.e. at the slopes of Mt. Etna, Italy, concentrations of up to 180 µg V L^{-1} have been recorded.

Vanadium is a redox-sensitive element, which occurs in three oxidation states (+III, +IV and +V) in the environment. Whereas vanadium(V) usually occurs as the oxyanion vanadate(V) under most environmental conditions, vanadyl(IV) is an oxocation that is stable at low pH and/or mildly reducing conditions, particularly when the organic matter concentration is high. Vanadium(III), which is the least studied form of vanadium, occurs under strongly reducing conditions. All vanadium forms are strongly bound to environmental sorbents: vanadate(V) is bound as a bidentate complex to iron, aluminium, and titanium (hydr)oxides, and with a stronger affinity than that of orthophosphate (*o*-phosphate). Vanadyl(IV) is strongly complexed to natural organic matter, while vanadium(III) may substitute for other trivalent ions in mineral structures. Despite this, vanadium may be mobilized to the aqueous phase, for example under high-pH conditions. Studies with V K-edge XANES spectroscopy have shown that most oxic soils usually contain a mixture of vanadium(IV) that is octahedrally coordinated in primary minerals, and surface-bound vanadate(V) on iron and aluminium (hydr)oxides, although acid organic soils are dominated by organically complexed vanadyl(IV). In reduced environments, such as in sediments and black shales, available evidence suggests that the V consists of a mixture of organically complexed vanadyl(IV) and unknown vanadium(III) species. However, considerable uncertainty exists on the V speciation under reducing conditions, and additional research is recommended.

Vanadium is essential for some species of cyanolichens and algae due to its presence in vanadium nitrogenase, which can be important for N fixation in boreal ecosystems, and in vanadium haloperoxidases, which mediate the oxidation of halides, particularly iodine and bromine. In certain organisms vanadium is accumulated for unknown reasons, e.g. in ascidians, where V accumulates as a vanadium(III) complex with organic S, and in *Amanita* mushrooms, in which amavadin, a stable vanadium(IV)-organic complex, is accumulated. However, at high concentrations vanadium is toxic to many organisms. This is mostly due to its interference with *o*-phosphate in a number of biomolecules. Available evidence shows that toxic effects appear in the mg V L^{-1} range for most studied species. However, some organisms, i.e. algae and possibly some soil bacteria, are more sensitive. In soils, the toxic response is related to the soil solution V concentration, rather than to the solid-phase concentration. The *o*-phosphate concentration has been identified as a parameter that influences toxicity, but the relationship between the P status and the environmental risk of V toxicity is not yet well determined – as a result risk-based guidelines remain uncertain. There is urgent need for more research on this topic.

Vanadium, being a redox-sensitive element, responds to sudden environmental change such as flooding that leads to decreased redox potential. In most, but not all, cases, an increased solubilisation of vanadium is observed after flooding, which can be attributed to reductive dissolution of vanadate(V)-sorbing iron (hydr)oxides and to vanadate(V) reduction to vanadyl(IV) that forms stable complexes with dissolved organic matter. The vanadium redox conversions are carried out by a large number of genera of bacteria. Bioremediation methods

* Department of Soil and Environment, Swedish University of Agricultural Sciences, Box 7014, 750 07 Uppsala, Sweden.
E-mail address: jon-petter.gustafsson@slu.se.

https://doi.org/10.1016/j.apgeochem.2018.12.027
Received 31 October 2018; Received in revised form 21 December 2018; Accepted 24 December 2018
Available online 14 January 2019

are being developed that may reduce vanadate(V) to vanadyl(IV), which may reduce the bioavailability of vanadium in many soils.

1. Introduction

Due to human activities, a large number of metals are released which may be potentially harmful to the environment at high concentrations. One such metal is vanadium, which, however, has been less studied than e.g. copper, zinc and lead in environmental research. Therefore, the knowledge about the environmental effects of vanadium is still relatively scarce.

From an environmental perspective, the interest in vanadium stems mostly from the increased dispersion of vanadium compounds in the biogeosphere, and the increased risk of toxic effects that this may cause. A well-known example of an incident from recent years is the accidental release of red mud in Ajka, Hungary, 2010. The red mud was a waste of aluminium production which, in addition to its high alkalinity and salt content, also contained elevated levels of vanadium (900 mg kg^{-1}) (Ruyters et al., 2011). Another example comes from Lillpite, Northern Sweden, where in 1990 the death of 24 heifers was related to vanadium poisoning from feed contaminated with a soil improver known as K-lime (a product that roughly corresponds to today's LD slag), which contained 3% vanadium (Frank et al., 1996). A similar incident was reported from South Africa, where eight cattle died after a vanadium mine dam collapsed close to where they were grazing (McCrindle et al., 2001). The increased use of heavy petroleum products with a high vanadium content, such as the oil sands of Alberta, Canada, and an accelerated exploration of vanadium-containing ores to meet demands in high grade steel and in the application of vanadium redox-flow batteries are all factors that are projected to increase the annual global fluxes of vanadium (Schlesinger et al., 2017; Watt et al., 2018), causing humans and other organisms to be increasingly exposed to vanadium.

Vanadium is an element in Group 5B of the periodic table. Its atomic number is 23 and it has the symbol V. Vanadium belongs to the same group as niobium (Nb) and tantalum (Ta). The atomic weight of vanadium is 50.95 g mol^{-1}. Naturally occurring vanadium is a mixture of two isotopes, ^{51}V (representing 99.76%) and ^{50}V (0.24%), of which the latter is weakly radioactive.

Elemental vanadium is a soft white metal, with a melting point of 1710 °C. It has a good resistance to both acids and bases. It oxidizes spontaneously at a temperature of about 660 °C. Common oxidation states of vanadium in nature are +III, +IV and +V. Vanadium(II) compounds are also found, but vanadium(II) is not thermodynamically stable at temperatures and pressures typical of the Earth's surface, see Chapter 2.

Vanadium was discovered twice in the early 19th century, first in 1801 by the Spanish-Mexican mineralogist Andrés Manuel del Río (1764–1849) in lead ore from Zimapán. He called the new element panchromium (*pancromo*, "all colours" in Greek) due to the multitude of colours it formed when exposed to different reagents, but he later changed its name to erythronium (from Greek *erythrosis*, meaning red). The German mineralogist Alexander von Humboldt, who visited Mexico at the time, was, however, skeptical about del Río's claim, believing it to be chromium, which had already been discovered. To settle the dispute, the sample was sent to the French researcher Hipplolyte-Victor Collet-Descotils for identification. Descotils agreed with von Humboldt that del Río had not found a new element, and that del Río had mistaken it for chromium. After learning about this, del Río recalled his discovery (Caswell, 2003).

Vanadium was discovered a second time in 1830 by the Swedish physician and chemist Nils Gabriel Sefström (1787–1845) when he, together with Jöns Jacob Berzelius (1779–1848), examined cast iron from ore mined at Taberg, south of Jönköping, Sweden, which contained vanadium pentoxide. Because of the beautiful colours, Sefström and Berzelius gave the new element the name *vanadium*, after the goddess Vanadis, another name for Freyja, the Nordic goddess for love and beauty. Berzelius sent some of the sample to the German chemist

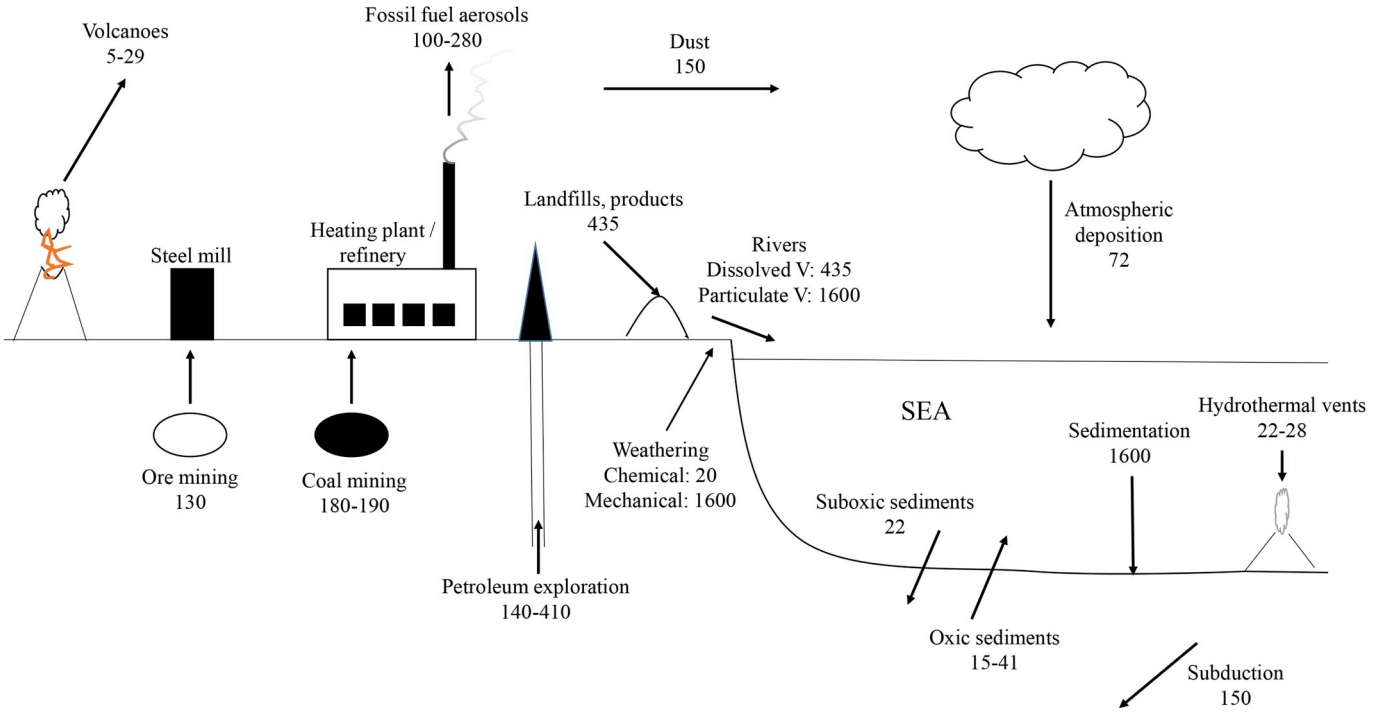

Fig. 1. Global biogeochemical cycle of vanadium (after Schlesinger et al., 2017). Annual fluxes are given in Gg V yr^{-1}.

Friedrich Wöhler, who had also obtained del Río's sample. In 1831, Wöhler proved that vanadium and erythronium were indeed the same new element. Despite the fact that the original discovery was made by del Río, the name of the element was to remain vanadium.

The purpose of this paper is to review current research developments concerning the low-temperature geochemistry of vanadium in the environment, with particular emphasis on vanadium speciation and on solid-solution interactions. The global occurrence and distribution of vanadium in different environmental compartments is treated only rather briefly in the current review. For more details on these aspects, the recent review by Huang et al. (2015) can be recommended. Two other significant sources of complementary information include a review on the biology of vanadium, written by Rehder (2015), as well as a quantitative analysis of the global biogeochemical cycle of vanadium, recently presented by Schlesinger et al. (2017). Parts of this paper can be seen as an update of the report by Gustafsson and Johnsson (2004), in which the then available thermodynamic data for vanadium compounds in the environment were reviewed.

2. Vanadium in the environment – occurrence and geochemistry

2.1. Global biogeochemical cycle of vanadium

Fig. 1 shows an overview of the annual fluxes in the global biogeochemical cycle of vanadium; it represents a slight simplification based on the recent compilation by Schlesinger et al. (2017), which in turn is based in part on the earlier works of Hope (1994, 2008). As is clear from the figure, the modern biogeochemical cycle of vanadium has a significant anthropogenic component, which mainly is a result of mining and petroleum exploration. Approximately 130,000 ton of vanadium is mined every year, according to an estimate of Monakhov et al. (2004). The most common use of vanadium is as alloy steel, often in combination with chromium, nickel, manganese, boron and tungsten. The global production of V metal has approximately doubled in the past 15 years, primarily because of increased demand for high-grade steel; this led to a 100% price increase in mined V during 2017 (Watt et al., 2018). Vanadium is also a trace contaminant in coal, which explains the high annual figure resulting from coal exploration (Fig. 1). Further, vanadium is a trace contaminant of petroleum products, particularly in the heavy fractions of raw oil. Combustion of fossil fuels, particularly oil, leads to a large annual release of vanadium as aerosols, amounting to between 100 and 280 Gg yr^{-1} (Fig. 1). A large part of the mined vanadium is stored in landfills and in products. The 'natural' biogeochemical vanadium cycle is dominated by the riverine transport of mechanically weathered, particulate V, and the sedimentation of this V in the oceans. A mean residence time of 100,000 yrs has been estimated for V in oceans (Whitfield and Turner, 1978).

The use of stable isotopes (i.e., $^{51}V/^{50}V$ isotope ratios) represents a potentially powerful tool for studying the biogeochemical cycle of V. However, sufficiently precise analytical methods have been developed only recently (Nielsen et al., 2011, 2016; Prytulak et al., 2011), and this research field is therefore still in its infancy. So far only rather small fractionations have been observed, e.g. up to 2‰ for crude oils (Ventura et al., 2015; Gao et al., 2017). Ventura et al. (2015) found a relatively broad range of $\delta^{51}V$ values of crude oils ranging from −1.64 to −0.22‰. This may reflect different redox conditions when the oil was formed. Seawater has a homogeneous isotopic composition with $\delta^{51}V = 0.20 \pm 0.15$‰ (Wu et al., 2018). A number of minerals has also been investigated, with a variation in $\delta^{51}V$ values of up to 1.5‰ (Wu et al., 2016; Schuth et al., 2017). Theoretical calculations predicted that the lighter ^{50}V isotope is preferentially adsorbed to goethite, resulting in substantial isotopic fractionation (Wu et al., 2015), but this still needs to be verified.

2.2. Vanadium in the Earth's crust

The average content of vanadium in the upper part of Earth's crust is estimated to 97 mg kg^{-1}, which is relatively similar to the concentration in bulk Earth (McDonough and Sun, 1995). The V concentration in the Earth's crust is approximately twice as high as for copper and 10 times higher than for lead (Nriagu, 1998). Vanadium levels are high in iron ore (between 600 and 4100 mg kg^{-1}) and apatite ore (from 10 to 1000 mg kg^{-1}). For example, in Swedish iron ore the range of V contents is usually between 1100 and 1300 mg kg^{-1}. Crude oil contains between 3 and 257 mg kg^{-1} (Nriagu, 1998). However, concentrations of up to 900 mg kg^{-1} have been reported for oil from Venezuela (Kabata-Pendias, 2001). As already mentioned, the vanadium is concentrated in the heavier oil fractions; this has been explained as a result of its association with high-molecular organic compounds (Lewan, 1984). Spectroscopic studies show that the main part of the vanadium is present as stable vanadyl(IV)-porphyrin complexes, which have a low solubility in organic solvents. This explains why they accumulate in the heaviest fractions (Dechaine and Gray, 2010). For example, asphaltene may contain up to 5400 mg V L^{-1} (López et al., 1995). Hence, the increased exploration of heavy petroleum products, for example from the Athabasca oil sands, may lead to increases in the anthropogenic vanadium emissions in the future (Schlesinger et al., 2017).

At the high temperatures that exist in the subsurface a multitude of V oxidation states may be stable (+II, +III, +IV and +V). For this reason there are also a large number of mineral phases that contain vanadium in their structures. Of particular importance is the fact that both V^{3+} and V^{4+} may substitute for Al^{3+} or Fe^{3+} in octahedral sites in a variety of minerals. This is the case, e.g. in titanomagnetites, which is a commercially important host phase for vanadium (Balan et al., 2006). The redox speciation of vanadium has also been used to indicate the oxygen fugacity of the melt (Sutton et al., 2005).

More than 80 minerals in the bedrock contain V (Nriagu, 1998). They may divided into a number of groups as follows:

- *Sulphides.* Among these are, for example, patronite, VS_4, and sulvanite Cu_3VS_4.
- *Sulphates.* Examples include minisragrite, $VOSO_4 \times 5H_2O$ and cheremnykhite, $Pb_3Zn_3TeO_6(VO_4)_2$.
- *Silicates.* An example is roscoelite, $K(V,Al,Mg)_2AlSi_3O_{10}(OH)_2$. This is an example of a mineral where the vanadium is found as V^{3+} in the octahedral layer. As mentioned above, vanadium(IV) can also be found in the octahedral layer of silicate minerals, examples where this is the case are kaolinite and sepiolite (Gehring et al., 1993, 1994).
- *Oxides.* Navajoite, $V_2O_5 \times 3H_2O$, montroseite $(V^{3+}, Fe^{3+})OOH$
- *Phosphates.* Vanadate is able to enter solid solutions with apatite, due to its ability to substitute for the *o*-phosphate anion (Boechat et al., 2000). An example of an apatite-type mineral is vanadinite, $Pb_5(VO_4)_3Cl$. In vanadinite, vanadate(V) has replaced phosphate because of the structural similarity between vanadate and phosphate.
- *Vanadates.* Some examples are chervetite, $Pb_2V_2O_7$, tyuyamunite, $Ca(UO_2)_2V_2O_8 \times 5–8H_2O$, calcium vanadate hydrate, $CaV_2O_6 \times 4–5H_2O$, carnotite, $K_2(UO_2)_2(VO_4)_2 \times 3H_2O$, and volborthite, $Cu_3V_2O_7(OH)_2 \times 2H_2O$.

Some of these minerals, e.g. vanadinite, may form and dissolve at equilibrium, which render them important for the short-term cycling of vanadium, see section 2.4.

2.3. Vanadium in soils

The vanadium content in soils is governed by the mineralogical composition of the parent material. The mean vanadium content in soils has been estimated to 108 mg kg^{-1} (Edwards et al., 1995), but most

regional surveys suggest lower values. For example, in European topsoils, the median total V concentration is 60.4 mg kg^{-1}, with a range from 1.28 to 537 mg kg^{-1}, according to the FOREGS database (De Vos and Tarviainen, 2006). Subsoils were slightly higher in V, i.e. the median total V concentration was 62.8 mg kg^{-1}. Shacklette and Boerngen (1984) obtained a value of 84 mg kg^{-1} for American soils. In European soils, there is a strong relationship with total Fe and total Sc, particularly in subsoils (De Vos and Tarviainen, 2006). Cappuyns and Slabbinck (2012) found that a multiple regression model containing total Fe, total Al and total Mg could explain 84% of the variation in total V for floodplain soils in the FOREGS data set.

Soils developed in black shales usually have comparably high V concentrations due to the enrichment of V under the euxinic conditions in which they were formed (Tribovillard et al., 2006). Worldwide, the average V concentration in black shales has been estimated to 790 mg kg^{-1} (Chermak and Schreiber, 2014), with maximum values of up to 2540 mg kg^{-1} (Scott et al., 2017). Finally, when interpreting values for pseudo-total V by e.g. aqua regia, it is important to note that for vanadium, aqua regia will only extract about half of the total V (De Vos and Tarviainen, 2006).

If V deposited from human activities is significant, one would expect enrichment with respect to V in the surface horizon of soils. For soils from a catchment in Pennsylvania, Kraepiel et al. (2015) collected litterfall, O horizon material, and mineral soil and compared the cycling of a range of different metals including V. Vanadium showed a similar behaviour as Cr, with increasing concentrations with increasing soil depth. The geochemistry of these metals was influenced mostly by weathering with little detectable influence of biological activity or of atmospheric deposition. Similarly, Guagliardi et al. (2018) determined total V in 149 topsoil samples in southern Italy and found no evidence for accumulation of V due to human activities in urban vs. rural areas. Nevertheless there are soils that have been subject to considerable vanadium contamination. These include soils in China polluted by vanadium and coal mining as well as by smelting operations, in which vanadium concentrations up to 4800 mg V kg^{-1} have been determined (Xiao et al., 2015; Cao et al., 2017). Another example is the area around a vanadium titanomagnetite mine in South Africa, where the soils contained between 1570 and 3600 mg V kg^{-1} (Panichev et al., 2006). Further, in the Mexican city of Salamanca there is strong evidence for vanadium accumulation relative that of the surrounding rural areas due to the presence of heavy industry (Hernandez and Rodriguez, 2012).

2.4. Vanadium in natural waters

2.4.1. Vanadium in precipitation, groundwaters, rivers and lakes

The vanadium concentration in precipitation is highly variable. A large number of data were compiled by Schlesinger et al. (2017), who found that in remote areas, the volume-weighted V concentration ranged from 0.0005 to 0.2 μg V L^{-1}, whereas in areas with moderate to high human activity, the V concentration ranged from 0.2 to 5.1 μg V L^{-1}. Krachler et al. (2003) investigated long-term V accumulation in a Swiss peat bog, and found that atmospheric soil dust is the predominating source of V in precipitation. Further, when normalized to Sc, they found that V deposition was remarkably constant until the onset of industrial revolution. When the results were combined with an earlier study on V in ice cores from Antarctica (Planchon et al., 2002), they estimated a modern-day enrichment factor of V relative to background to 4.0 for the period 1959 to 1990. However, in a Scottish peat bog, it was found that the anthropogenic V deposition (corrected for soil dust) reached a peak in the 1950s, after which it has decreased about fivefold (Cloy et al., 2010). This might be due to reduced atmospheric emissions in Europe. Consistent with this is the decrease in V deposition as reflected in moss between 1990 and 2000 (Harmens et al., 2007).

The concentration of vanadium in groundwater, rivers and lakes depends both on the atmospheric deposition and on weathering of the bedrock in the catchment area. Again the dissolved concentration of vanadium is highly variable. The average vanadium concentration in Californian groundwater is 5 μg V L^{-1} according to the survey of Wright and Belitz (2010). The highest concentrations were observed where the groundwater was alkaline and/or oxic. In many areas in the world the vanadium concentration is considerably lower. For example in Sweden, the median concentration of vanadium in bottled mineral water was 0.39 μg V L^{-1} (Rosborg et al., 2005).

However, in areas where the bedrock is vanadium-rich, concentrations may be significantly higher than the concentrations stated above. Mt. Fuji in Japan consists of vanadium-rich basalts. Here the groundwater often contains between 10 and 20 μg V L^{-1}. Deep groundwater may contain up to 147 μg V L^{-1} (Hamada, 1998). Similarly, the Mt. Etna groundwater in Italy is high in vanadium (Minelli et al., 2000), and in some drinking water sources the V concentration is as high as 180 μg V L^{-1}, which may pose a health risk (Arena et al., 2015).

Rivers and lakes differ in a similar way in terms of their dissolved V concentrations. Gardner et al. (2017) assembled a large number of data from small mountainous rivers and rivers draining high standing islands in different parts of the world. In an area in Taiwan dominated by metamorphic rocks, the median V concentration was 0.1 μg V L^{-1} whereas it was 65 μg V L^{-1} in rivers draining volcanic rocks in Nicaragua. In European stream waters, the median value is 0.46 μg V L^{-1} according to the FOREGS database (De Vos and Tarviainen, 2006), and in five Norwegian reference lakes the median V concentration was 0.40 μg V L^{-1} (Borg, 1984).

Johannesson et al. (2000) investigated dissolved vanadium concentrations in a number of Sierra Nevada rivers. Dissolved V varied between 0.5 and 24 μg V L^{-1} depending on location and sampling time. High V concentrations were associated with high weathering rates, alkaline conditions, and evaporation. However, there were also evidence for considerable V sorption in the stream beds, especially during periods of stagnant flow.

Often the concentration of dissolved vanadium in rivers appears to be correlated to silicon, with an average V/Si ratio of 66×10^{-6}, which indicates that the dominant source of dissolved vanadium is silicate weathering (Shiller and Mao, 2000). Recent studies by Gardner et al. (2017) confirmed that V is strongly correlated with Si in catchments dominated by igneous silicate rocks. However, in sedimentary regions, this trend was not observed. Furthermore, most of the river-borne vanadium is bound to particles or colloids. Based on statistics and size fractionation techniques, iron oxide-containing colloids were found to govern vanadium transport in rivers in NW Russia and in Sweden (Pokrovsky and Schott, 2002; Stolpe et al., 2005; Wällstedt et al., 2010); this was explained by their ability to form strong surface complexes with vanadate(V). By contrast, Pourret et al. (2012) and Shi et al. (2016) found that vanadium in waters was related to dissolved organic matter, suggesting instead vanadyl(IV) to be an important dissolved phase. However, it appears difficult to base conclusions on vanadium speciation on statistical comparisons, even if accompanied by size fractionation, as there is often considerable co-variation of e.g. iron and dissolved organic matter (Wällstedt et al., 2010). Therefore, direct speciation is probably a more reliable approach for distinguishing between the different dissolved vanadium phases, see chapter 2.4.4.

The exact role of colloidal and particulate V for the riverine V transport on a global scale is still poorly known. According to the estimate shown in Fig. 1, the flux of dissolved V in riverine input to the ocean is only between 0.5 and 2% of the total V flux (from Hope, 2008, based on data of Dobrovolsky, 1994).

2.4.2. Vanadium in seawater

The mean concentration of sea water has been estimated to 1.8 μg V L^{-1} (Schlesinger et al., 2017), but the concentration is variable. For example, in the English Channel the concentrations are between 0.5 and 1 μg V L^{-1} (Auger et al., 1999), and in the Landsort Deep of the Baltic Sea the dissolved V was only about 0.15 μg V L^{-1} (Bauer et al.,

2017). In a large section of the East Pacific, dissolved V was between 1.3 and 1.4 μg V L^{-1}, but somewhat higher (1.8 μg V L^{-1}) near the Peru Margin (Ho et al., 2018). The surface water of the East Pacific is about 5% lower in V than the deeper waters, which may be due to biological uptake and incorporation into particulate V, which is higher at the surface (Ho et al., 2018).

In some cases it has been observed that reducing conditions, which may occur in bottom waters, lead to lower V concentrations. This may be due to the reduction of vanadate to lower oxidation states (vanadyl or V^{3+}), which are then retained in the sediment (Shiller and Mao, 1999). Adsorption of vanadate to sedimentary iron oxides can also help to bind vanadium into the sediment (Auger et al., 1999). The latter process has been evidenced in particular for hydrothermal vents, where dissolved V decreases, probably due to vanadate(V) adsorption to iron (hydr)oxides formed in these environments (Ho et al., 2018; see also Fig. 1). In the Landsort Deep of the Baltic Sea, dissolved V remained relatively constant with depth, but with a distinct minimum in the redox transition zone (between the oxic surface water and the anoxic bottom water), where particulate V increased, possibly due to an adsorption or coprecipitation mechanism with Mn(III) (Bauer et al., 2017).

2.4.3. Aquatic chemistry of vanadium

In the environment, vanadium occurs in four different oxidation states, +II, +III, +IV (i.e. vanadyl) and +V (usually vanadate). The divalent oxidation state, i.e. V(II), is thermodynamically unstable in water, but in certain cases it may be present in crystalline mineral phases formed at high temperature, or possibly in certain organic complexes where V(II) is stabilized thanks to its strong binding. The redox conditions determine which species that dominates. In order to correctly understand the water chemistry of vanadium, it is important to have access to reasonably correct thermodynamic data for the various reactions that can occur. In this review, particular attention has been paid to the following compilations of thermodynamic data for vanadium species:

1. Cruywagen (1999). Protonation and oligomerization constants for vanadate(V), which in turn were based on data reported by, among others, Larson (1995) and Elvingson et al. (1996).
2. NIST Critical Stability Constants Database 46. This database contains recommended equilibrium constants for different vanadium species, but is not updated anymore. The last version was No. 8.0 (Smith et al., 2004).
3. Wanty and Goldhaber (1992). Compilation of water chemistry for vanadium (III), vanadyl(IV) and vanadate(V) species. However, this database is based on fewer and older data than sources 1 and 2 above.
4. McCann et al. (2013, 2015). These authors reviewed some of the oligomerization constants for vanadate(V) and supplied additional entries including vanadate(V)-carbonate species.
5. Buglyó et al. (2005). Derived vanadium(III) hydrolysis constants from a set of titrations.
6. Allison et al. (1991). The MINTEQA2 database contains a number of vanadium-containing solid phases.

To produce the figures in this section, Visual MINTEQ 3.1 was used (Gustafsson, 2018), with vanadium equilibrium constants that were selected from the above databases (Table 1, Tables S1–S4, Supporting materials).

As concerns the vanadium redox equilibria, the two investigated databases, i.e. of Wanty and Goldhaber (1992), and of Allison et al. (1991) are in reasonable agreement (Table 1). These equilibria, and the equilibrium reactions described below, can be used to draw an Eh-pH diagram, an example of which can be seen in Fig. 2 for a total V concentration of 1 μmol L^{-1}. Under these conditions, the aqueous speciation of V is dominated by vanadate(V) at high pH and at high redox potentials at low pH, whereas vanadyl(IV) is stable at low pH and at intermediate redox potentials. At low redox potential, vanadium(III) is stable. Vanadium(II), occurring as V^{2+}, is not stable inside the stability boundary of water. In vanadium redox-flow batteries practical use is made of these redox equilibria. In the negative half-cell, V^{2+} is oxidized to V^{3+} when the electrons migrate to the positive half-cell, in which VO_2^+, i.e. oxovanadium(V), is reduced to VO^{2+}. When the system is charged, the electrons flow in the opposite direction (Li et al., 2011).

Vanadium(III) is expected to be stable under strongly anoxic ('euxinic') conditions, such as in sulphide-containing sediments and wetlands. The cation $V(H_2O)_6^{3+}$ is octahedrally coordinated with a mean V−O bond length of 1.992 Å (Krakowiak et al., 2012), which means that its coordination environment is similar to that of Fe^{3+} and also has a similar water chemistry.

The thermodynamic data for vanadium(III) hydrolysis that are currently used in geochemical models such as Visual MINTEQ should be considered uncertain. For example, in Table S1, the results from the single data set of Buglyó et al. (2005) is shown to be considerably different from the selected data from the NIST compilation. The data of Buglyó et al. (2005) are in better agreement with the iron(III) hydrolysis constants (assuming that vanadium(III) hydrolysis is similar), but they represent a rather narrow range of conditions. Because of the latter, the NIST compilation remains the basis for Visual MINTEQ speciation. However, as the hydrolysis constants of V(III) are still rather poorly constrained there is clearly a need for a more thorough evaluation. In any case, according to the selected data, V^{3+} hydrolyses to VOH^{2+} at pH 2.3 at zero ionic strength, and is then hydrolysed one step further to $V(OH)_2^+$ at pH 4.7. At high pH values, the solubility of vanadium(III) may be restricted by various precipitates if dissolved V is sufficiently high. In Fig. 2, precipitation of $V(OH)_3$(s) occurs at pH > 6.9, which brings down the total V concentration to less than 1 μmol L^{-1}. Further, vanadium(III) forms strong complexes with fluoride and with sulphate (Table S1), and it is likely that it also is complexed strongly to a range of different organic ligands including humic substances.

Vanadium(IV) occurs in solution as the oxovanadium(IV) or vanadyl (IV), VO^{2+}, which is characterized by its strong V=O bond, with a bond length of 1.588 Å (Krakowiak et al., 2012). Vanadyl(IV) is stable in moderately reducing environments, especially under acidic conditions. Organic surface horizons in forest soils, *Sphagnum* peat bogs, and surface waters with low pH values, are examples of environments where vanadyl(IV) is probably the most stable vanadium species. Vanadyl(IV) is the most stable oxocation in a natural environment (Wehrli and Stumm, 1989). The special configuration also provides part of the explanation as to why vanadyl(IV) is highly reactive and forms a large number of strong complexes with inorganic and organic ligands, some listed in Table S2. As implied by the selected hydrolysis constants in Table S2, VO^{2+} is hydrolyzed to $VOOH^+$ at pH 5.7. At least theoretically, the solubility of vanadyl(IV) can be limited by the hydroxide VO$(OH)_2$(s). In reality, however, precipitation of $VO(OH)_2$(s) is probably

Table 1
Redox equilbria for the conversions between the four different redox species of vanadium. Values in bold were selected for Visual MINTEQ.

Redox couple	Reaction	Allison et al. (1991)		Wanty and Goldhaber (1992)	
		E^0 (V)	log *K*	E^0	log *K*
HVO_4^{2-}/VO^{2+}	$HVO_4^{2-} + 5H^+ + e^- \leftrightarrow VO^{2+} + 3H_2O$	**1.90**	**32.08**	1.88	31.79
VO^{2+}/V^{3+}	$VO^{2+} + 2H^+ + e^- \leftrightarrow V^{3+} + H_2O$	**0.34**	**5.70**	0.34	5.70
V^{3+}/V^{2+}	$V^{3+} + e^- \leftrightarrow V^{2+}$	**−0.25**	**−4.31**	–	-

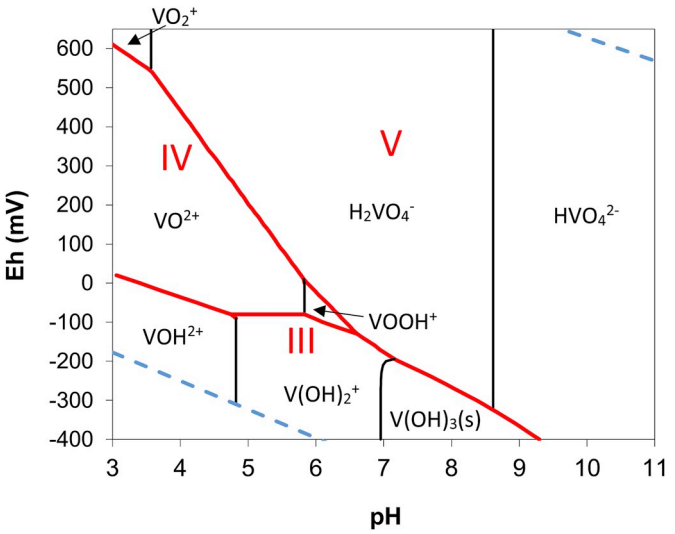

Fig. 2. Predominance diagram showing the vanadium speciation as a function of pH and Eh at total dissolved V = 1 μmol L^{-1}. T = 25 °C, I = 0.01 mol L^{-1} (as NaCl). The red solid lines separate the predominance fields of the three oxidation states III, IV, and V. The blue dashed lines represent the stability lines of water with respect to $H_2(g)$ (at low Eh) and $O_2(g)$ (at high Eh). To produce the diagram, equilibrium constants selected for Visual MINTEQ were used (Tables 1, S1, S2 and S3). (For interpretation of the references to colour in this figure legend, the reader is referred to the Web version of this article.)

unusual, due to the fact that vanadyl(IV) forms such strong complexes with many ligands.

Dissolved vanadium(V) occurs in different coordination environments depending on the pH. At very low pH (< 3.6), vanadium(V) is present as the vanadyl(V) cation VO_2^+, while at higher pH it is present as the tetrahedral vanadate(V) ion $H_nVO_4^{(3-n)-}$. Vanadate(V) is often compared to *o*-phosphate, which has broadly similar acid-base characteristics and a similar coordination environment. However, there are a number of distinct differences. First, there is no evidence for the existence of orthovanadic acid, H_3VO_4, at low pH, instead there is a direct transition from tetrahedral $H_2VO_4^-$ to the oxocation VO_2^+ at pH 3.6. Second, the ion size of vanadate(V) is considerably larger; the inner-shell V—O bond length is 1.72 Å whereas it is 1.54 Å for the corresponding P—O distance (Krakowiak et al., 2012). Further, the pK_a values of $H_2VO_4^-$ and HVO_4^{2-} are slightly larger than the ones of $H_2PO_4^-$ and HPO_4^{2-} (8.8 and 13.5 compared to 7.2 and 12.4). Molecular dynamics simulations show that HVO_4^{2-} is very probably associated with Na^+ in seawater (Priest et al., 2017), but thermodynamic data for this interaction are still missing.

Vanadate(V) forms oligomers at high V concentrations. Dimers, i.e. $H_nV_2O_7^{(2-n)-}$, account for a certain proportion of the dissolved vanadium (V) although they never become predominant. Perhaps more importantly, at V concentrations above 10^{-4} M and at low pH, the decavanadates $HV_{10}O_{28}^{5-}$ and $V_{10}O_{28}^{6-}$ will be the most thermodynamically stable vanadium(V) species (Fig. 3). These will completely dominate the V speciation when total V > 10^{-3} M and if pH is below 6. At higher pH, i.e. between 6 and 9, dodecavanadates, above all $V_4O_{12}^{4-}$, will be the dominating vanadium(V) species when total V > $10^{-2.5}$ M. In the decavanadates and dodecavanadates, vanadium (V) is no longer tetrahedrally coordinated but will instead be present in a distorted octahedral configuration.

Vanadium(V) forms a series of complexes with both inorganic and organic ligands at low pH, when VO_2^+ is quantitatively important (c.f. Table S3). Complexation with e.g. organic ligands occurs also at higher pH, when vanadate(V) becomes predominant. Ceci et al. (2015) found that saprotrophic fungi are able to dissolve vanadinite by a mechanism that involves oxalate, which complexes vanadate(V) and contributes to mineral dissolution. Vanadate reacts readily with carboxyl and hydroxyl groups to form esters, in a similar way as *o*-phosphate (Rehder, 2015). However, when pH < 6, vanadate(V) is also easily reduced to vanadyl(IV) in the environment, for example due to the reducing ability of humic substances (Lu et al., 1998). Also other organic acids such as oxalic acid may reduce vanadate(V) to vanadyl(IV) at low pH (Bruyère et al., 2001).

Precipitation of solid phases appear not to be a very important solubility-governing mechanism for vanadium, except in certain cases. For vanadium(III), as mentioned earlier, $V(OH)_3(s)$ can possibly be formed at relatively high pH. This hydroxide can then be recrystallized into the less soluble $V_2O_3(s)$. However, it appears likely that none of these in reality is common in the natural environment. This is due to the fact that vanadium(III) is readily incorporated into less soluble Fe and Al oxides and silicate minerals. Schwertmann and Pfab (1994, 1996) were the first to show that V^{3+}, due to its strong resemblance to Fe^{3+}, is able to enter the structure of iron oxides as a solid V + Fe oxide solution. As mentioned above, vanadyl(IV) is not likely to form stable precipitates. In the case of vanadate(V), solubility constants have been determined for a large number of vanadates (Table S4). It turns out, however, that almost all are very soluble and not readily formed in natural environments; e.g. the solubility of the specified calcium vanadates means that these are stable only in cement pastes and similar Ca-rich environments when pH > 12.5 (Huijgen and Comans, 2006). Potentially, these conditions could be met when alkaline steel slags, known to contain V(V) in Ca-rich mineral phases such as Ca ferrite, C2F, and di-Ca silicate, C2S (Presslinger and Klepp, 2002; van Zomeren et al., 2011), are subject to leaching. However, observations and model simulations suggest that secondary Ca vanadates do not form during slag leaching, and that dissolved V(V) is instead governed by the incongruent dissolution of the C2F and C2S phases, which accelerates at lower pH (Huijgen and Comans, 2006; De Windt et al., 2011; van Zomeren et al., 2011).

According to existing literature data, there are, however, some mineral phases that may be of significance in the natural environment. These include Ba and Pb vanadates (Table S4; Cornelis et al., 2008). One example is vanadinite, $Pb_5(VO_4)_3Cl(s)$. Vanadinite is an apatite-type mineral. Gerke et al. (2009) showed that precipitation of vanadinite can govern the solubility of Pb^{2+} and vanadate(V) in drinking water supplies, as it accumulates in pipe corrosion scales even at μg L^{-1}

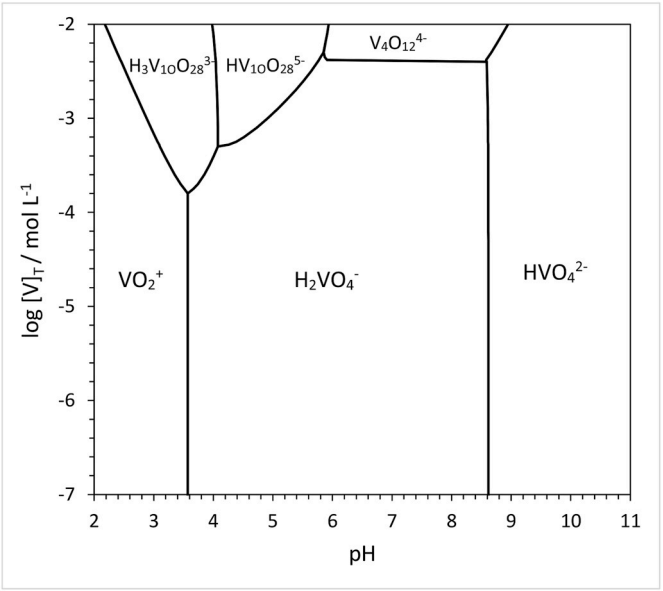

Fig. 3. Predominance diagram showing the speciation of vanadate (V) as a function of pH and total concentration of vanadium, $[V]_T$. T = 25 °C, I = 0.01 mol L^{-1} (as NaCl). To produce the diagram, equilibrium constants selected for Visual MINTEQ were used (Table S3).

levels of dissolved vanadium. They were also able to tentatively determine the solubility constants of the formed vanadinite, which is included in Table S4.

2.4.4. Vanadium speciation in waters and in soil extracts

As may be expected from the previous section, dissolved vanadium in most natural waters is a mixture of vanadyl(IV) and vanadate(V). Determination of the actual speciation is of interest for example because of its relevance for toxicity assessments: as mentioned elsewhere, vanadate(V) is considered the more toxic vanadium species due to its resemblance to *o*-phosphate. However, it is only during the last two decades that methods have been developed that allow the direct speciation of vanadium. The methods have been reviewed in detail by Pyrzyńska (2006) and by Chen and Owens (2008). Briefly, two families of methods can be distinguished, i.e. separation methods (often using liquid chromatography or capillary electrophoresis) and spectrophotometric methods. As for the latter, Chen and Owens (2008) mention six different chromogenic reagents that can be used. Irrespectively of the chosen technique, one problem is to achieve sufficiently low detection limits for the various V species.

Minelli et al. (2000) separated vanadyl and vanadate for a number of V-rich Italian waters using strong anion exchange columns treated with EDTA. The water samples had been collected from volcanic areas with basalts (Mt. Etna and Castelli Romani), where the dissolved V concentration was between 7 and 70 μg V L^{-1}. Between 30 and 40% existed as vanadyl(IV) in most of the water samples examined. Liu and Jiang (2002) used ICP-MS with a dynamic reaction cell (DRC) and achieved detection limits of 0.007 and 0.013 μg V L^{-1} for vanadyl(IV) and vanadate(V), respectively. The method was tested on four waters with total V concentrations between 0.3 and 0.9 μg V L^{-1}. One of the water samples was dominated by vanadyl(IV), the other three by vanadate(V). Aureli et al. (2008) developed the separation method of Minelli et al. (2000) further to an HPLC-ICP-MS method, allowing for a much improved sensitivity. They determined the V speciation for a number of bottled mineral waters and found that the vanadium was almost exclusively present as vanadate(V).

Wang and Sañudo-Wilhelmy (2009) separated V species with a Chelex 100 resin, and applied this method to study vanadium speciation in the Long Island Sound, US. They found that dissolved V ranged from 0.6 to 1.2 μg V L^{-1}, with the highest values during summer, and the lowest in spring. On average, between 85 and 90% of the V was vanadate(V), with the remainder being vanadyl(IV). However, in the western part of the Long Island Sound, vanadyl(IV) accounted for up to 40% of total V during spring. This was attributed to an influx of reduced V from sewage inputs.

The method of Aureli et al. (2008) was also used for the speciation of V in soil extracts. For example, Baken et al. (2012) showed that the vast majority of the $CaCl_2$-extractable V in soils subject to vanadium ecotoxicity studies was indeed vanadate(V). Moreover, Larsson et al. (2015b) showed that $CaCl_2$ extracts from an acid forest soil were dominated by vanadyl(IV) prior to the addition of vanadate(V)-containing converter lime. 25 years after the addition, the O horizon extracts were still dominated by vanadyl(IV), whereas soil extracts from the mineral soil were dominated by vanadate(V). In addition, Larsson et al. (2015a) showed that approximately the same redox speciation was obtained irrespectively of whether vanadate(V) or vanadyl(IV) had been added to soil samples one week prior to analysis, which indicated that the redox conversions were rapid. In addition, V in leachates from blast furnace slag was investigated and was found to be dominated by vanadyl(IV) (Larsson et al., 2015a).

Gamage et al. (2010) developed a vanadate(V)/vanadyl(IV) separation method based on an ion chromatograph-ICP-MS with a nitric acid mobile phase, obtaining detection limits of 0.02 μg V L^{-1} and 0.06 μg V L^{-1} for vanadyl(IV) and vanadate(V), respectively. They applied the method to study the V speciation in Sierra Nevada groundwaters (concentration range 3.7–82.1 μg V L^{-1}), and found that vanadate(V) accounted for 98–99% of total V.

Jensen-Fontaine et al. (2014) used a HPLC-ICP-MS method to study the V speciation in tissue extracts of *Hyalella azteca* after exposure for seven days of a solution consisting of a mixture of vanadate(V) and vanadyl(IV). During exposure, most of the vanadyl(IV) was oxidized to vanadate(V). The tissue extracts showed the presence of both vanadyl (IV) and vanadate(V), and in addition an unidentified V species, possibly a V(IV)-protein complex.

3. Biology and toxicity of vanadium

3.1. Essentiality of vanadium

For most organisms including mammals, vanadium is not known to have any essential biological function. However, vanadium is present in a large number of biomolecules. Two are of fundamental importance for certain forms of life:

3.1.1. Vanadium nitrogenase

Nitrogenase is an enzyme that catalyses biological nitrogen fixation (BNF), a mechanism responsible for up to 97% of N input in unmanaged terrestrial ecosystems (Vitousek et al., 2002). The main form of nitrogenase is Mo nitrogenase, whereas V nitrogenase has long been recognized as an 'alternative' nitrogenase, with an unclear role for BNF. The reaction that V nitrogenase catalyses is the reduction of N_2(g) to NH_4^+. The electrons required for this process are supplied by respiratory oxidation of organic C to CO_2. Recently, the structure of V nitrogenase was resolved (Sippel and Einsle, 2017). The structure is similar, but not identical to, that of Mo nitrogenase (Costa Pessoa et al., 2015; Sippel and Einsle, 2017). In the active center of the enzyme, V occurs in a distorted octahedral configuration, bound to homocitrate, an amino acid, and to three adjacent iron atoms through three sulphur atoms (George et al., 1988; Costa Pessoa et al., 2015; Sippel and Einsle, 2017). The oxidation state of V has been subject to some discussion (i.e. to what extent it is V(II) or V(III)), but models of the electronic structure suggest the oxidation state to be +III (Costa Pessoa et al., 2015; Rees et al., 2017). On the whole, current research has shown.

V nitrogenase to be a less efficient catalyst than Mo nitrogenase, and it is also more easily degraded (Rees et al., 2017). However, a unique feature of V nitrogenase is its ability to also reduce CO efficiently (Sippel and Einsle, 2017).

Cyanobacteria of the *Anabaena* sp. and *Nostoc* sp. genera, as well as the soil bacteria *Azotobacter vinelandii* and *A. chroococcum*, are known to use V nitrogenase for N fixation (Costa Pessoa et al., 2015). Indeed, two recent papers by Darnajoux et al. (2014, 2017) show that the cyanolichen *Peltigera aphthosa* is dependent on N fixation through V nitrogenase, which is carried out by cyanobacteria that exist in the so-called cephaloida of the lichen. This may be the case also in other cyanolichens, which suggests that V nitrogenase may be more important for N_2 fixation in forest ecosystems than previously recognized.

3.1.2. Vanadate-dependent haloperoxidases

This group of enzymes, abbreviated VHPOs, catalyze the oxidation of halides by H_2O_2 by a so-called bi-bi ping-pong mechanism (Leblanc et al., 2015). The exact structure depends on the halide to be oxidized. In general, the enzymes consist of $H_2VO_4^-$, i.e. dihydrogen vanadate (V), which is bound to a nitrogen group of histidine and is further stabilized through hydrogen bonding to amino acid residues (Rehder, 2015). The VHPOs are used by a variety of bacteria and fungi. For example, the fungi *Curvularia inaequalis* oxidatively degrades lignocellulose in the cell wall of their host. In this process, a VHPO releases HOCl, a short-lived intermediate, which carries out the oxidative attack (Messerschmidt and Wever, 1995; Rehder, 2015). Moreover, the VHPOs are believed to have a key role for the biogeochemical cycling of iodine (and also for bromine) in the environment. For example, they mediate the formation of iodocarbons in kelps (Leblanc et al., 2006).

This process leads to the volatilization of iodine compounds from the sea, which constitute an important source of iodine in the terrestrial environment.

In addition, several groups of bacteria are able to use vanadate(V) as an electron acceptor for redox reactions. Further, the bacterium *Pseudomonas isachenkovii* is able to use vanadium instead of molybdenum in nitrate reductase (Antipov et al., 1998).

3.2. Nonspecific accumulation of vanadium

A number of organisms have been shown to take up and accumulate vanadium in their biomass, for reasons that are still not clear. The most well-known example is ascidians such as *Ascidia gemmata*, which has been shown to have V concentrations up to 350 mmol L^{-1} (Rehder, 2015). The ascidians take up vanadate(V) from sea water, which is then reduced to vanadium(III), c.f. section 4.2.2. Mushrooms of the *Amanita* genus are also able to accumulate vanadium. In this case the vanadium is reduced to vanadyl(IV), which is then complexed to N-hydroxyimino-2,20-diisopropionate ("hidpa") ligands, resulting in so-called amavadin, which may possibly may be an evolutionary relic of a peroxidase (Berry et al., 1999; Rehder, 2015). The biological role of amavadin is still unclear, although it is known to be a good catalyst for a range of different reactions (da Silva et al., 2013). In amavadin, vanadium(IV) is no longer an oxocation, but is present as a "naked" 8-coordinated complex with six oxygen and two nitrogen ligands (Bayer et al., 1987; Berry et al., 1999). Strong accumulation of V has also been observed in cyanobacteria of the *Trichodesmium* genus, collected in the Sargasso Sea (Nuester et al., 2012). V:C ratios ranging from 66 to 100 μmol mol^{-1} were recorded, which were up to fourfold higher than the Fe:C ratios. It could not be identified what mechanisms that were responsible for the V accumulation, but the authors hypothesized that the V was related to N fixation, either through V nitrogenase or indirectly through other enzymes such as VHPOs.

3.3. Microbially mediated redox reactions of vanadium

Microbes mediate the vanadium redox conversions, and in some studies the genera responsible for these reactions have been identified. For example *Pseudomonas* strains are able to reduce vanadate(V) (Lyalkova and Yurkova, 1992). Also Shewanella oneidensis was found to reduce vanadate(V) to vanadyl(IV) in an anaerobic environment, using lactate, formate and pyruvate as electron acceptors (Carpentier et al., 2003). Efficient reduction of vanadate(V) to vanadyl(IV) were also obtained using the chemolithotrophs *Acidithiobacillus ferrooxidans* and *Acidithiobacillus thiooxidans* (Bredberg et al., 2004). The latter authors argued that the method could be used to extract vanadium from oil ash and from spent catalysts. Zhang et al. (2015) found efficient reduction of vanadate(V) (up to 87%) when anaerobic sludge was used as inoculated seed. In this case dissimilatory reduction was carried out by *Lactococcus* and *Enterobacter* with oxidation of lactic and acetic acid from fermentative microorganisms.

3.4. Vanadium ecotoxicity

Ecotoxic effects from vanadium stem primarily from the similar structure of vanadate(V) and *o*-phosphate, and thus from the interference with the function of P-containing biomolecules. Many phosphatase enzymes, which catalyse the hydrolysis of organophosphate ester bonds, are inhibited by vanadate(V), probably by its ability to form a complex at the active site of the enzyme (Seargeant and Stinson, 1979; Crans et al., 2004). For these reasons, vanadate(V) is the most toxic form of vanadium. In line with this, practically all information on the ecotoxicity of vanadium in soils and waters results from experiments in which vanadate(V) salts were added.

Smit (2012) provided a summary of the literature on ecotoxicity for vanadium in water. Above all certain algae respond to vanadate(V) additions, but the effect is highly variable depending on the species and on the strain. In the studies of Lee et al. (1979) and Nalewajko et al. (1995a, 1995b), which are important sources of V ecotoxicity data for algae, the NOEC (no observed effect concentrations) range from < 1 μg V L^{-1} to several mg V L^{-1}. Although some of the data can be questioned, these studies indicated that some algae were particularly sensitive to vanadate(V). Based on these data, Smit (2012) suggested a long-term maximum permissible concentration (MPC) for the Netherlands of 1.2 μg V L^{-1}, which is only slightly higher than the estimated natural background for Dutch waters (0.82 μg V L^{-1}).

Schiffer and Liber (2017a, 2017b) determined acute and chronic toxicity for a wide range of aquatic organisms in reconstituted Athabasca river water. The most sensitive species in their study was *Daphnia dentifera*, for which an EC20 value of 80 μg V L^{-1} was found. For the most sensitive algae an LOEC value of around 100 μg V L^{-1} was obtained. According to Nalewajko et al. (1995b) and Schiffer and Liber (2017a), the sometimes very low NOEC values of Lee et al. (1979) and Nalewajko et al. (1995a, 1995b) were probably impacted by P-deficient conditions in the test solutions, which led to increased effects of vanadate(V) due to competition for uptake sites. Schiffer and Liber (2017b), on the other hand, used an axenic nutrient solution in their test medium, with a P concentration of 0.12 mg P L^{-1}. They then obtained a 5th percentile of the species sensitivity distribution (HC5) of chronic V toxicity at 50 μg V L^{-1}. The difference between the results of Smit (2012) and Schiffer and Liber (2017b) illustrate not only that a critical review of test conditions is key to successful extraction of risk-based guidelines for V, but also that additional studies are desirable to more precisely determine the ecotoxicity of V in waters especially as a function of P availability.

For soils, it has been known for a long time that vanadium inhibits soil microbiota at high concentrations, for example by inhibiting nitrogen mineralisation and nitrification. Liang and Tabatabai (1977, 1978) showed that both nitrogen mineralisation and nitrification rates were affected at a V dose of approximately 250 mg V kg^{-1}. As concerns the potential nitrification rate, Larsson et al. (2013) obtained EC10 values ranging from 2.2 to 190 mg V kg^{-1} for five different soils, while the EC10 values for substrate-induced respiration ranged from 8.4 to 58 mg V kg^{-1} for the same soils. The sometimes low values suggest that some soil bacteria are quite sensitive to vanadium. In line with this, Sun et al. (2018) recently showed that the rhizosphere microbiota responded more strongly to V (and Cr) contamination than to other metal contaminants such as Cu, Cd, Pb, and As in multimetal(loid)-contaminated soils.

However, Wilke (1989) argued, based on his results, that such effects may be transitory and may at least partly decrease in the long term because of adaptation. Tyler (1976) showed that the soil phosphatase activity was inhibited when the V concentration exceeded 100 mg V kg^{-1}. By contrast, Yang et al. (2014) could not observe any inhibitions on the soil phosphatase activity; instead they observed effects on sulphatase and phenol oxidase activities, usually with 50% reductions at around 100 mg V kg^{-1}.

As for plants, early studies showed that ecotoxic effects usually started to appear at soil solution concentrations of 1–10 mg V L^{-1}, which is much higher than the dissolved V concentrations that usually occur in natural soils (Kaplan et al., 1990a, 1990b; Carlson et al., 1991; Gil et al., 1995). Vanadium mainly accumulates in the roots, and there is a linear relationship between soil labile V and the root V concentration (Qian et al., 2014). For barley root length, barley shoot growth and tomato shoot growth, Larsson et al. (2013) obtained EC50 values in the range from 0.8 to 13.4 mg V L^{-1} for five different soils, which is consistent with these results. This was equivalent to added V concentrations ranging from 18 to 510 mg V kg^{-1}. The EC10 values were slightly lower (11–250 mg V kg^{-1}). Biomass reduction by collard was observed at 80 mg kg^{-1} for a sandy soil, but for a loamy sand no effect was seen at 100 mg kg^{-1}, which was the highest dose (Kaplan et al., 1990b). The growth of soybean seedlings was affected between

30 and 75 mg kg^{-1}, depending on the soil (Wang and Liu, 1999).

The latter results show that soil properties are influential for the toxic response. This was further examined by Larsson et al. (2013), who studied vanadate(V) effects on barley root elongation in five different soils. When adding the results from all five soils to the same dose-response plot, the results were consistent only when the dose was expressed in mg V L^{-1}, while considerable scatter occurred if expressing the V dose in mg kg^{-1}. A similar result was obtained when plotting the total V concentration in plant biomass as a function of pseudo-total V and of dissolved V, showing much better correspondence with the latter (Fig. 4, Larsson et al., 2015a). Finally, the EC50 value was related to the Freundlich sorption strength, for three different sets of data (Larsson et al., 2013). The authors concluded that the V toxicity is dependent on the amount of V taken up, which is determined by the solubility of vanadate(V) in the soil, which in turn is dependent on the extent of V sorption to solid particle surfaces such as Fe(III) and Al(III) (hydr) oxides (Larsson et al., 2013, 2015a). This is supported by results of Zhang et al. (2018b), who found that addition of zero-valent iron to vanadium-contaminated soils reduced V uptake to Canola plants, leading to an increased plant biomass.

Mišik et al. (2014) showed that red mud caused chromosomal damage in *Tradescantia* (spiderwort) and in the root cells of *Allium* plants. These toxicity symptoms appeared at a solution concentrations of around 1 mg V L^{-1}, and the toxic effects were explained by the elevated levels of V in the red mud.

For four plant species, Smith et al. (2013) found that the fertilization level had a dramatic effect on the toxic response to vanadium(IV). For example, for lettuce (*Lactuca sativa*) the EC25 value increased from 4 to 120 mg V kg^{-1} when the fertilization level increased from 1 to 100 kg ha^{-1} as 20:20:20 (N:P:K) fertilizer.

Baken et al. (2012) investigated the effect of ageing, where ecotoxic effects were compared for soils that had been spiked with vanadate(V) immediately before seeding ("freshly spiked") with soils that had been spiked 330 d before seeding ("aged"). It was found that the aged soils had EC50 values that were, on average, 1.9 times higher. This was associated with lower V solubility over time. These results are consistent with similar effects observed for other metals (Smolders et al., 2009). The explanation behind the ageing effect is unclear, but may be due to slow sorption or diffusion reactions.

Reports of ecotoxic effects resulting from additions of vanadium compounds other than vanadate(V) are scarce, but Larsson et al. (2015a) examined the effect of varying additions on blast furnace slag (with total V = 800 mg kg^{-1}) to soil on barley shoot growth, 10 months after spiking. No effects were observed that could be explained by V toxicity. This was attributed to the low solubility of V in the slag.

There are studies that show that small additions of V, below the toxicity threshold, may instead have a beneficial effect on plant growth. A recent example is provided by García-Jiménez et al. (2018), who found that an addition of 5 µmol V L^{-1} increased the growth and flowering of pepper plants. The mechanisms are, as yet, unknown. However, higher V additions (10–15 µmol V L^{-1}) led to toxic effects. This suggests that for some organisms, there can be quite a narrow optimal range of V concentrations.

3.5. Remediation of vanadium-contaminated soils

Where vanadium is a contaminant of concern, it is of interest to devise remedial measures to decrease the toxicity and leaching of this element. Lehoux et al. (2013) studied the effect of gypsum addition to red mud-contaminated soils in Hungary. Application of gypsum decreased the pH value from between 8.5 and 11 to between 7.5 and 8.5. This led to a much lower dissolved V concentration, reducing both bioavailability and the risk for leaching. Another way to decrease dissolved V is to apply bioreduction methods. Ortiz-Bernad et al. (2004) found that injection of acetate, which worked as an electron donor, stimulated the growth of *Geobacter metallireducens* bacteria capable of reducing vanadate(V) to vanadyl(IV) in V-contaminated aquifers, which decreased the V mobility. Bioreduction can also be carried out with hydrogen as the sole electron donor (Jiang et al., 2018). With this method the genera *Dechloromonas* and *Hydrogenophaga* were both capable of reducing vanadate(V) to vanadyl(IV), again decreasing dissolved V in contaminated groundwater. Recently it was also found that elemental sulphur and zerovalent iron can be used as electron donors causing efficient microbial reduction of vanadate(V) to vanadyl(IV) (Zhang et al., 2018a).

4. Vanadium species in the solid phase

As vanadium has three oxidation states (III, IV, and V) which can all be stable in the environment, vanadium speciation is a challenging task. However, to understand the geochemistry of vanadium, and to be able to design models to predict its solubility and bioavailability, correct information from speciation studies is essential.

Almost all reported results concerning the direct determination of vanadium species in the solid phase of environmental materials are from XAS (X-ray absorption spectroscopy) conducted at the vanadium K edge at 5465 eV. Most of these studies have employed vanadium K-edge XANES (X-ray absorption near edge structure) spectroscopy. This is

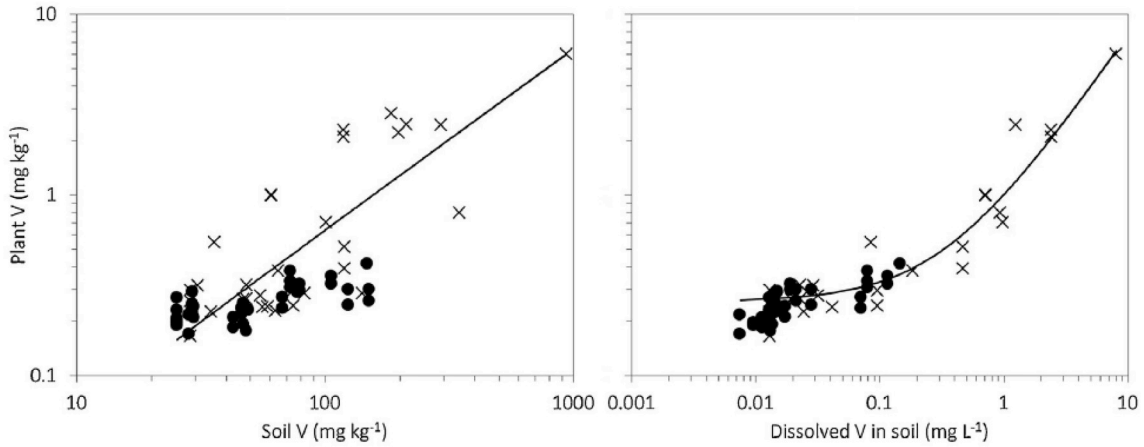

Fig. 4. Barley shoot concentration of vanadium as a function of the pseudo-total vanadium concentration, in mg V kg^{-1} (left) and in the dissolved phase, in mg V L^{-1} (right). The data are from two different soils, Pustnäs and Säby, which were treated with vanadate (**x**), and with two different blast furnace slags, M-kalk and Merit 5000 (●). Linear regression lines, plotted on a log-log scale, were fitted to the whole data set, R^2 = 0.72 (left, n = 71) and R^2 = 0.95 (right, n = 64). From Larsson et al. (2015a).

partly due to the fact that the vanadium K edge is relatively rich in features, as explained below in section 4.2. Moreover, the EXAFS (extended X-ray absorption fine structure) region is subject to interferences from other elements, which makes the use of EXAFS difficult for most environmental materials. Probably the most serious interference is from Ba, as demonstrated by Huggins et al. (2000). They showed that the Ba L_2 edge at 5624 eV interrupted the V K-edge EXAFS region. Fig. 5 presents an example of a V K-edge X-ray absorption spectrum from one of the soils used by Larsson et al. (2017b). As the Ba L_2 edge arrives already at $k = 6$ Å^{-1} in the V K-edge EXAFS region, the information gained from EXAFS spectroscopy would not be practically useful. At high La concentrations, La may interfere with the interpretation of both XANES and EXAFS data, as the La L_3 edge is located at 5483 eV (Thompson et al., 2009). For a group of samples from red mud leachate residues and sediments, Burke et al. (2013) showed this effect to be significant, making linear combination fitting (LCF) of V K edge XANES data impossible. There may also be an interference from Ti, due to the fact that the Ti K edge is at an energy only 480 eV less than the V K edge. This means that in Ti-rich samples there may be a high level of background scatter that affect V K edge EXAFS data. Although the V K-edge XANES data are probably less sensitive to the Ti effect, effects have been reported (Bennett et al., 2018).

For pure phases such as Fe (hydr)oxides none of these interferences are expected, and for this reason the determination of e.g. structures of surface complexes can be readily made using EXAFS spectroscopy.

4.1. Vanadium surface complexes on iron and aluminium (hydr)oxides

Iron(III) and aluminium(III) (hydr)oxides are usually considered as being of major importance for the sorption of oxyanions such as *o*-phosphate, arsenate and vanadate(V) in the environment (e.g. Dzombak and Morel, 1990; Wehrli and Stumm, 1989) So far, however, only two studies have been conducted that has focused on the characterization of these surface complexes with EXAFS spectroscopy, and both concerns vanadate(V) on iron(III) (hydr)oxides.

Peacock and Sherman (2004) conducted a pioneering study on the coordination of vanadate(V) on goethite at three different pH:s (3, 6, and 8). They concluded that corner-sharing bidentate complexes probably predominated at all investigated pH:s, as indicated by second-shell V···Fe distances of ~3.25 Å (Fig. 6, right). Additional evidence for edge-sharing bidentate complexes were found (with V···Fe = 2.80 Å; Fig. 6, left), but considered to be an artefact of the existence of multiple scattering paths within the VO_4 tetrahedron. This was backed up by DFT calculations showing that corner-sharing bidentate complexes were the most energetically favourable. Peacock and Sherman (2004) then constrained a surface complexation model based on these results, c.f. section 5.1.

A similar study was made by Larsson et al. (2017b) for the vanadate (V)-ferrihydrite system. In this case clear evidence for the predominance of an edge-sharing bidentate complex with V···Fe ~2.80 Å was found. This was supported also by results from Morlet wavelet transform (WT) analysis. To explain the apparent contradiction between the two studies, Larsson et al. (2017b) hypothesized that the different coordination modes were a result of different crystal structures on the surfaces of the two iron(III) (hydr)oxides. Ferrihydrite, having a larger number of singly coordinated FeOH groups that can form ^{1}E (edge-sharing bidentate) complexes, would thus be expected to host a larger proportion of the latter (Hiemstra, 2013). Additional evidence for this also comes from the investigation of other oxyanions such as molybdate and arsenite, for which similar trends are apparent (Gustafsson and Tiberg, 2015; Ona-Nguema et al., 2005).

In connection to the study carried out by Larsson et al. (2017b), additional EXAFS spectra were collected for vanadate(V) on amorphous Al hydroxide, which are shown here for the first time. The synthesis conditions and characterization of the amorphous Al hydroxide were reported by Larsson et al. (2015a), and the experimental conditions such as sorbate to sorbent ratios, background electrolyte (0.01 M $NaNO_3$) and equilibration time were identical to the ferrihydrite system (Larsson et al., 2017b). The EXAFS spectra shown in Fig. 7 could be well described by a model that contained a second-shell V···Al path at ~2.55 Å, and two different multiple scattering paths (V—O—O and V—O—Al) (Table S5, Supporting materials). Because of the slightly lower quality of these spectra as compared to the ferrihydrite spectra the Morlet WT:s were slightly less conclusive but nevertheless indicated little or no contribution from longer V···Al paths (Fig. S1, Supporting materials). In other words, the predominance of an edge-sharing bidentate complex is suggested also for vanadate(V) on amorphous Al hydroxide. This may not be surprising given the amorphous nature of the sorbent, which should lead to the presence of many singly coordinated AlOH groups at the surface.

So far, no studies have been published in which the structures of the surface complexes that vanadyl(IV) forms with iron(III) and aluminium (III) (hydr)oxides have been evaluated with spectroscopic approaches.

Vanadium K-edge EXAFS spectroscopy was used also by Kaur et al. (2009) to determine the conditions under which V^{3+} may substitute for Fe^{3+} in goethite, evidence for which was obtained already by Schwertmann and Pfab (1994, 1996). The former authors found that large amounts of V^{3+} (up to 13 mol %) can be substituted if goethite is synthesized at low temperature (< 25 °C) and when reducing conditions are maintained. If not, V^{3+} was oxidized to V(IV) and V(V).

4.2. Vanadium speciation in environmental materials as evidenced by XANES spectroscopy

4.2.1. Methodology

The vanadium K edge contains a number of features in the XANES region, and these provide information on the oxidation state and symmetry of the vanadium in the sample. The different features that are observed are due to the different electronic transitions that occur when an electron is excited from the K shell. An important feature is the so-called pre-edge feature, which can be strong for vanadium in higher oxidation states (III and higher). Moreover, the position of the main absorption edge depends, in a general sense, on the oxidation state (Fig. 8). The pre-edge feature (feature I in Fig. 8) is due to 1s → 3d electronic transitions, which are normally not allowed. Therefore, there is no pre-edge feature for vanadium(0) metal, for which 1s → 4p dipole-allowed transitions predominate completely. The same is true for vanadium(II) oxide, which has perfect octahedral symmetry (Wong et al., 1984). However, vanadium(III) and vanadium (IV) oxide (i.e., V_2O_3(s)

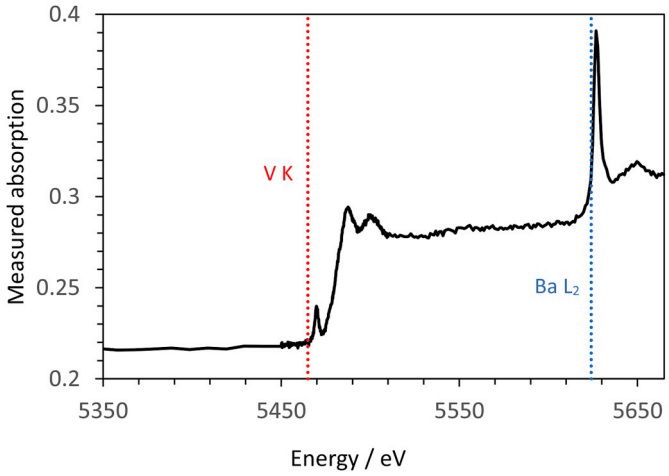

Fig. 5. X-ray absorption spectrum of the Säby soil (no added V; c.f. Larsson et al., 2017a, for details on the sample). The dotted lines show the position of the V K and Ba L_2 edges at 5465 and 5624 eV, respectively (Thompson et al., 2009).

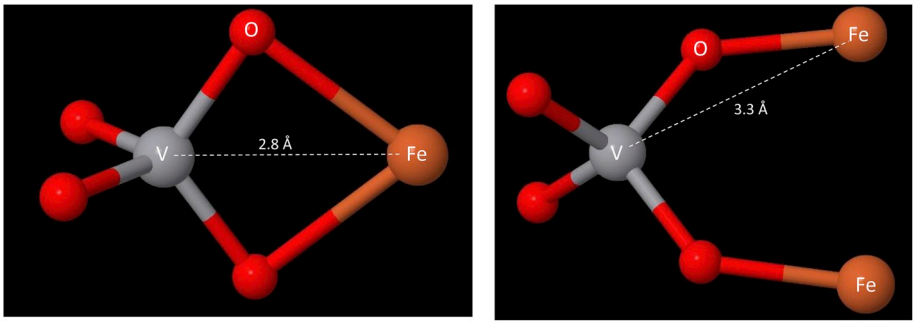

Fig. 6. Jmol ball-and-stick images showing an edge-sharing bidentate complex of vanadate(V) on iron (hydr)oxide (left) and a corner-sharing bidentate complex (right). The approximate V···Fe distances are shown.

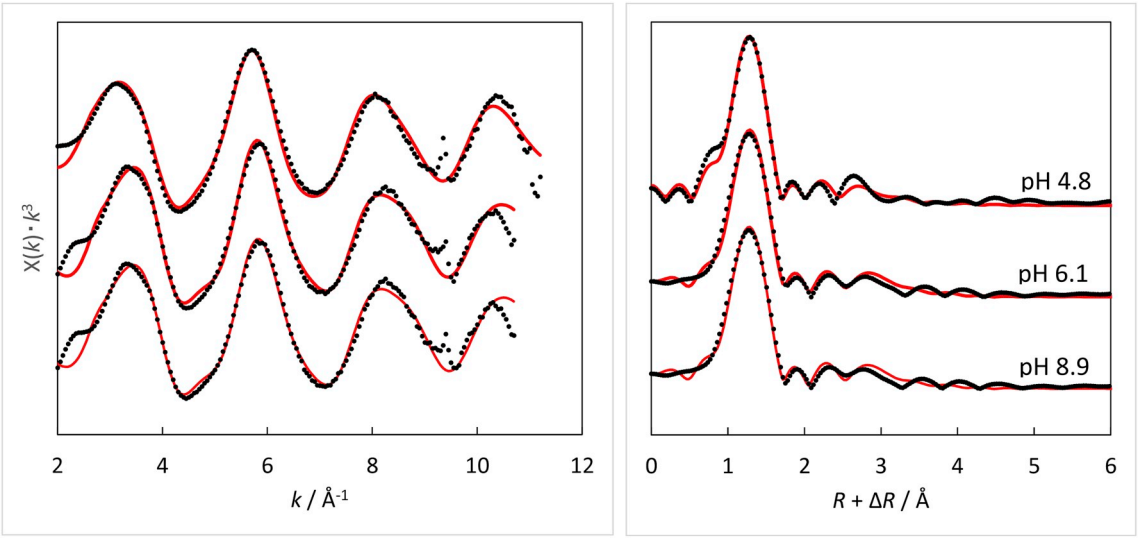

Fig. 7. Left: stacked k^3-weighted V K-edge EXAFS spectra for vanadium sorbed to amorphous aluminium hydroxide at three different pH values. Right: stacked Fourier transform magnitudes of the k^3-weighted EXAFS spectra. Black and red lines represent experimental data and fits, respectively (see Table S1 for the models used to produce the fits). (For interpretation of the references to colour in this figure legend, the reader is referred to the Web version of this article.)

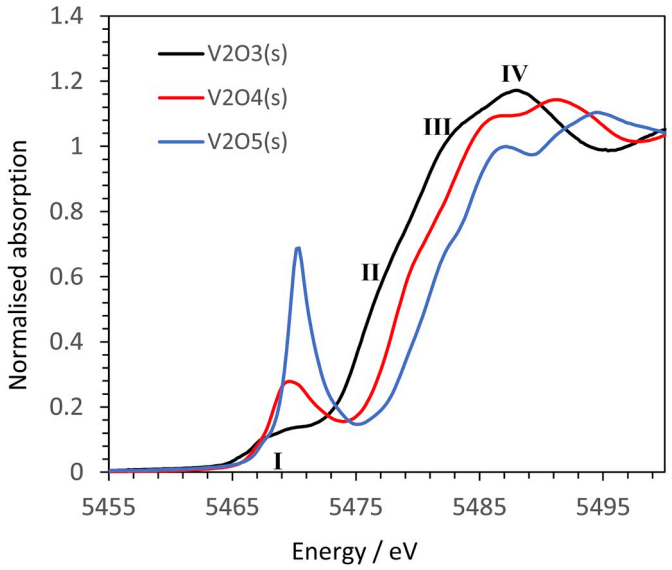

Fig. 8. Normalized vanadium K-edge XANES spectra for V_2O_3(s), V_2O_4(s) and V_2O_5(s). Roman numerals show approximate energy positions of electronic transitions for the V_2O_3(s) reference, as follows: I: 1s → 3d, II: 1s → 4p shakedown, III: 1s → $4p_z$, IV: 1s → $4p_{xy}$.

and V_2O_4(s)) form distorted octahedra, where the 3d and 4p orbitals hybridize, which allows for 1s → 3d transitions (Wong et al., 1984; Kelly et al., 2008). In vanadium(V) oxide as well as in vanadyl(IV) compounds (such as dissolved $VOSO_4$, see Fig. 9), vanadium has square-pyramidal coordination, which leads to an even stronger pre-edge feature. Vanadium(V) can also be tetrahedrally coordinated, as in aqueous VO_4^{3-}, which also has a strong pre-edge feature (Fig. 9).

Further, the 1s → 4p transitions, which occur at and around the main absorption edge, can be divided into at least three different features, which can be seen as shoulders or peaks on the edge (II, III and IV in Fig. 8). These are the 1s → 4p showdown, 1s → $4p_z$ and 1s → $4p_{xy}$ transitions, respectively. Depending on the V oxidation state and symmetry, these features may be of varying significance and located at different energies on the edge.

A number of authors have tried to use these features to develop models for estimating the mean oxidation state of vanadium in environmental samples. Sutton et al. (2005) suggested the use of the pre-edge peak intensity to predict the mean oxidation state using a polynomial. Although the authors recognized that the pre-edge peak intensity is dependent not only on oxidation state, but also on symmetry, they nevertheless found a strong relationship with the pre-edge peak intensity when they used references of the same composition as the samples (which were glasses). Chaurand et al. (2007b) developed a more complex model where both the centroid position of the pre-edge feature and the E½ value of the main edge (i.e. the energy at which the normalized absorption equals 0.5) are taken into account. Larsson et al.

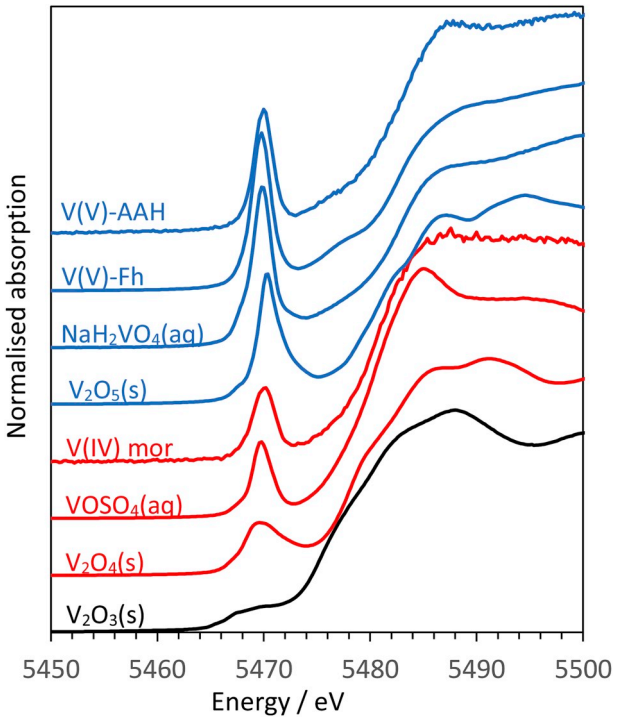

Fig. 9. Vanadium K-edge XANES spectra of the references used by Larsson et al. (2015a; 2017a). Black: vanadium(III), red: vanadium(IV), blue: vanadium(V). V(V)-Fh: vanadate(V) on ferrihydrite; V(V)-Fh: vanadate(V) on amorphous Al $(OH)_3$(s). (For interpretation of the references to colour in this figure legend, the reader is referred to the Web version of this article.)

(2015a, 2015b) used only the E½ value of the main edge in their model, as consideration of the pre-edge feature did not improve the model. On the other hand, Levina et al. (2014) developed the approach of Chaurand et al. (2007b) further to predict the mean oxidation state from three-dimensional parameter plots where the pre-edge peak energy, the pre-edge peak height, the main edge energy, and the white-line intensity were all taken into account.

To estimate the vanadium speciation with XANES spectroscopy, the most commonly employed method so far has been LCF, which requires the use of a number of references thought to be representative for the endmembers of the sample. These types of calculations are often carried out using Athena (Ravel and Newville, 2005). Examples of such studies include those of Gerke et al. (2009), Larsson et al. (2015b; 2017a) and Wisawapipat and Kretzschmar (2017), and the results are discussed in the next section. To some extent this approach to vanadium speciation can be considered empirical, as the endmembers (references) are taken directly from measurements, and then Athena calculates the combinations that provide the best fit. Progress is currently being made on how to predict V K-edge XANES spectra for compounds with known structures (Benzi et al., 2016). Another future development is the complementary use of X-ray emission (XES) techniques, which have some additional information content (Rees et al., 2016).

4.2.2. Vanadium speciation in different environmental samples

Table 2 summarizes the results from a number of studies in which solid-phase speciation of V has been estimated using V K-edge XANES spectroscopy and related techniques. On the whole, the number of studies is, as yet, quite limited. So far it is soils and some products/by-products and waste materials such as coke and slags that have been most frequently studied. On the other hand, only two studies were found that used XANES spectroscopy for V speciation in reduced natural samples (Bennett et al., 2018; Nedrich et al., 2018). For this and many other types of samples, there are more published papers reporting the results from chemical extractions (see section 3.3).

As concerns living organisms, Patrick Frank and colleagues determined V speciation in ascidians in a number of pioneering papers (e.g., Frank et al., 1998; Frank et al., 2003; Frank et al., 2008; Frank et al., 2014). Their studies showed that vanadium(III) was the dominating oxidation state in the blood cells, but that vanadyl(IV) contributes as well. In *Ascidia ceratodes*, the presence of a vanadium(III) $-SO_4$ complex appeared to be a major sink for vanadium (Frank et al., 1998, 2003). Based on their findings, Frank et al. (2008) proposed the existence of a vanadium reductase in the blood cells of the ascidians. The active site of the reductase is hypothesized to have a ligand array similar to that of EDTA. A nearby carboxylic acid residue helps to activate the vanadyl(IV) ion towards reaction, whereas a thiol binding site near the active site mediates the reduction to 7-coordinate vanadium (III). By use of S K-edge XANES spectroscopy, Frank et al. (2014) later discovered that the vanadium(III)$-SO_4$ complex that they proposed was an artefact of the freezing step during sample preparation, and that the exact nature of the accumulated 7-coordinated vanadium(III) species is not known, although at very low pH (< 1.5) vanadium(III) forms complexes with sulphonate groups of sulphate esters.

In the mycelium *Phycomyces blakesleeanus* vanadium speciation depended on the species that was applied (c.f. Table 2; Žižić et al., 2015). In a follow-up study using ^{51}V NMR spectroscopy, it was shown that added vanadate was complexed intracellularly, possibly with polyphosphate compounds (Žižić et al., 2016).

Larsson et al. (2015a, 2015b, 2017a) studied vanadium speciation by use of XANES spectroscopy in a number of Swedish forested and agricultural soils. In an acid forest soil to which vanadate-containing converter lime had been added in the 1980s, the added vanadium was recovered mostly as vanadyl(IV) in the mor layer (the organic surface horizon). Deeper down in the soil profile the vanadium appeared to have accumulated as vanadate(V), but particularly at greater depth the native content of vanadium, consisting mostly of octahedral vanadium (IV), dominated (Larsson et al., 2015b). Three other soils, two A horizons from agricultural soils and one B horizon from a Podzol, were spiked with 2.25 mmol kg^{-1} vanadate(V) on the laboratory (Larsson et al., 2015a, 2017a). Prior to the additions the mean V oxidation states of these soils ranged from 3.7 to 4.2, apparently due to the presence of a multitude of native V phases with oxidation states III, IV and V. After the vanadate(V) additions, the V oxidation state consistently increased. LCF suggested that almost all of the added vanadate(V) had been adsorbed to iron(III) and aluminium(III) (hydr)oxides including allophane, and that very little V reduction had taken place (Larsson et al., 2017a). Addition of vanadyl(IV) instead of vanadate(V) led to similar aqueous vanadium speciation as evidenced by HPLC-ICP-MS, suggesting that most vanadyl(IV) was oxidized to vanadate(V) and then adsorbed (Larsson et al., 2015a).

Wisawapipat and Kretzschmar (2017) studied V speciation in a group of highly weathered soils from Thailand in which the total V content was high, i.e. between 200 and 600 mg kg^{-1}. According to LCF, most of the V appeared to be bound to kaolinite, either as octahedral vanadium(IV) in the kaolinite structure or as adsorbed vanadate(V). In addition there were evidence for adsorbed vanadate(V) on iron (hydr) oxides (ferrihydrite and goethite). In some soils the LCF results also indicated a contribution of "V(V) adsorbed to iron(III)-humic complexes".

Terzano et al. (2007) studied vanadium speciation in an Fe-rich industrially polluted soil by a combination of methods including μ-XANES spectroscopy, μ-XRF (X-ray fluorescence) and μ-XRD (X-ray diffraction). Vanadium was mostly present as vanadate(V), of which the majority was vanadate adsorbed to hematite, whereas a minor proportion was identified as being present in the Cu-vanadate mineral phase volborthite, $Cu_3(OH)_2V_2O_7 \times H_2O$(s).

Limited spectroscopic information exists regarding the speciation of V in black shales, which are known to be enriched in V. The only XANES spectra that could be found in the literature were those of Sahoo (2015), who studied the Ediacaran Doushantuo shales, China. Here,

Table 2
Laboratory studies that have investigated the mean oxidation state and/or speciation of vanadium in solid environmental samples with spectroscopic methods.

Materials studied	Oxidation state and/or symmetry	Vanadium speciation	Method	Comment	Reference
Ascidia species (tunicates, $n = 3$), blood cells	No	Yes	XANES-LCF	(Frozen) blood cells of *A. ceratodes* are characterised by the importance of a vanadium (III)−SO_4 complex whereas in the blood cells of *Phallusia nigra*, most V is present as other unknown vanadium(III) species	Frank et al. (2003)
Phycomyces blakesleeanus mycelium ($n = 2$)	Yes	No	μ-XANES	Exposure of vanadate(V) led to accumulation of a mixture of tetrahedral V(V) and octahedral V(IV) in the vacuoles, whereas exposure of vanadyl(IV) caused accumulation of equal proportions of octahedral and square-pyramidal (vanadyl) vanadium(IV), in both cases with a minor contribution of V(III)	Žižić et al. (2015)
Soils ($n = 12$, Dystric Arenosol)	Yes	Yes	XANES-LCF	Range of mean oxidation states: 3.7–4.6, with lowest values for the mor layer where V was complexed as vanadyl(IV) to OM. In mineral soil horizons V was to a larger extent bound as vanadate(V) bound to Fe/Al or as vanadium(IV) in primary minerals	Larsson et al. (2015b)
Soils ($n = 4$, Cambisol and Regosol), blast furnace slag ($n = 2$)	Yes	No	XANES	Soils: range of mean oxidation states: 3.7–4.9, highest values recorded when vanadate(V) was added. Slags: dominated by vanadium(III).	Larsson et al. (2015a)
Soils ($n = 6$, Cambisol, Regosol, Podzol)	Yes	Yes	XANES-LCF	Range of mean oxidation states: 3.7–4.9, highest values recorded when vanadate(V) was added. XANES-LCF was carried out only for vanadate(V)-amended soils. For these, vanadate(V) adsorbed to ferrihydrite and $Al(OH)_3$ dominated the V speciation.	Larsson et al. (2017a)
Soils ($n = 20$, Oxisols)	No[a]	Yes	XANES-LCF	Vanadium(IV) bound in kaolinite, and vanadate(V) sorbed to kaolinite were prominent phases in most samples. Some samples also contained large proportions of vanadate(V)-sorbed humic substances, according to LCF.	Wisawapipat and Kretzschmar (2017)
Several thin sections from industrially polluted soil	Yes	Yes	u-XANES, u-XRF, u-XRD	Vanadium(V) predominated, most was associated with hematite (sorbed) or with magnetite. Some was present in the Cu−V(V) mineral volborthite.	Terzano et al. (2007)
Ediacaran black shales ($n = 8$)	Yes	No	XANES	Predominance of vanadium(III) in all samples	Sahoo (2015)
Marine sediment ($n = 1$)	Yes	Yes	XANES-LCF, SXRF	Mean oxidation state 3.5	Bennett et al. (2018)
River reservoir sediment ($n = 2$)	Yes	No	XANES-LCF	74% of the V could be attributed to a V_2O_3-type phase, i.e. V(III), and 26% to vanadium (IV).	Nedrich et al. (2018)
Fe−Ti oxides, natural and synthetic ($n = 22$)	Yes	No	HERFD-XANES	In titanomagnetite, the V(IV) content was 8–16%, the remainder being V(III). In hematite, V(IV) dominated	Bordage et al. (2011)
Titanomagnetite	Yes	No	XES-XANES	90% V(III) and 10% V(IV). Both occurred in the octrahedral site of the spinel structure.	Balan et al. (2006)
Vanadium(V)-doped birnessite ($n = 4$)	No	Yes	XANES, EXAFS, XRD	Predominance of vanadium(V), possibly as V_6O_{16} units sorbed on the birnessite	Yin et al. (2015)
Vanadium(V)-doped α-MnO_2 ($n = 2$)	Yes	Yes	XANES-LCF, EXAFS, XPS	Mix of tetrahedral and octahedral vanadium(V)	Chen et al. (2018)
Red mud ($n = 2$)	No	Yes	XANES	Vanadate(V) predominated	Burke et al. (2012)
Red mud ($n = 1$)	Yes	Yes	XANES	Vanadate(V) sorbed to Fe and/or Al (hydr)oxides	Burke et al. (2013)
Coal ($n = 4$)	No	Yes	XANES, EXAFS	Predominance of vanadium(V) in V2O4-like environment	Maylotte et al. (1981)
Blast furnace slags ($n = 2$)	Yes	No	XANES	Range of mean oxidation states: 3.0–3.2	Larsson et al. (2015a)
Blast oxygen furnace slag ($n = 49$)	Yes	Yes	u-XANES, u-XRF	Most samples contained predominantly tetrahedral vanadate(V), some V(IV), no sample contained V(III). The V(IV) was probably bound in the aluminoferrite.	Hobson et al. (2017)
Blast oxygen furnace slag ($n = 3$)	Yes	No	XANES	Predominance of vanadium(IV). The oxidation state decreased slightly following leaching (from 4.1 to 3.9) and increased during aging (to 4.3)	Chaurand et al. (2006), Chaurand et al. (2007a)
Pipe corrosion scales ($n = 20$)	No	Yes	XANES-LCF	In most samples, vanadinite predominated, with a minor (< 10%) contribution from vanadium(V) oxide	Gerke et al. (2009)
Pipe corrosion scales ($n = 5$)	No	Yes	u-XANES-LCF	Presents u-XANES results supporting the results from Gerke et al. (2009)	Gerke et al. (2010)
Bauxite residues ($n = 4$)	Yes	Yes	u-XANES	Oxidation state around 4 in 3 samples, closer to 3 in 1 sample. Most vanadium was probably associated with ilmenite and goethite.	Gräfe et al. (2011)
Oil sands petroleum coke ($n = 9$)	No	Yes	XANES-LCF	Three vanadyl porphyrins dominated the V speciation, with minor contributions (< 10%) from V(III)-containing roscoelite	Nesbitt et al. (2017a)

(*continued on next page*)

Table 2 (*continued*)

Materials studied	Oxidation state and/or symmetry	Vanadium speciation	Method	Comment	Reference
Petroleum coke	Yes	No	XANES	Vanadium(V) dominates under most conditions, except at low O_2 partial pressures and low Ca content, when vanadium(III) dominates	Duchesne et al. (2018)
Fluid petroleum coke deposits (n = 12)	No	Yes	u-XANES-LCF, u-XRF	Vanadyl porphyrins dominated in inner regions, whereas the outer margins contained up to 50% V(III)-containing roscoelite	Nesbitt and Lindsay (2017)
Bioreactors with Fe(0) and S(0) (n = 2)	Yes	No	XPS	A mixture of V(IV) and V(V) was identified	Zhang et al. (2018a)
Particulate matter from diesel emissions	No	Yes	XANES-LCF	In fine fractions, vanadium(V) oxide predominated. In coarser fractions, there was a mix between tetrahedral vanadate(V) and either vanadyl(IV) or vanadium(III).	Shafer et al. (2012)
Precipitates from alkaline slag leachate	Yes	Yes	XANES	Predominance of vanadate(V) bound to Fe(III) (hydr)oxides	Hobson et al. (2018)

[a] Although the authors derived relationships to calculate the mean oxidation state, no such results were reported in the paper.

vanadium(III) was found to be the predominant oxidation state, and the shape of the spectra was similar to that of roscoelite, where V(III) may substitute for Al(III) or Mg(II) in the structure. This observation is consistent with hypotheses put forward by Scott et al. (2017), who also obtained results that were in agreement with earlier ideas (e.g. Breit and Wanty, 1991; Wanty and Goldhaber, 1992), i.e. that V accumulation in shales are dependent on high H_2S concentrations, which may occur under euxinic conditions. According to this hypothesis, the high sulphide concentrations may reduce organically complexed vanadyl(IV) to octahedral vanadium(III), which enters mineral phases and becomes practically insoluble with time.

Until very recently, there were no spectroscopic studies in the literature showing the V speciation in freshwater or marine sediments. However, for a marine sediment from a coastal lagoon in Queensland, Australia, Bennett et al. (2018) found that vanadium was a mixture of the oxidation states III and IV, with an average oxidation state of +3.5. Reducing conditions were prevailing in this sediment, which is mirrored by the fact that Fe sulphide phases were identified. Complementary studies using scanning X-ray fluorescence microscopy (SXFM) indicated detrital organic matter to be the most important host phase for the vanadium. However, this assignment was uncertain due to the close proximity of the Ti Kβ and the V Kα emission lines. In another recent study, Nedrich et al. (2018) performed V K-edge XANES spectroscopy for two sediment samples from a river reservoir. In this case a predominance of vanadium(III) was found (74%), whereas the rest was present as vanadium(IV) (Nedrich et al., 2018). No efforts were made to determine the host phase for the vanadium in this freshwater sediment.

Vanadium-bearing Fe—Ti oxides constitute the most important host phase for commercial vanadium exploration. An example is the titanomagnetite found in the Bushveld complex, South Africa, which is the most important vanadium deposit in the world. The V speciation was investigated by Balan et al. (2006) and by Bordage et al. (2011), and was found to be dominated (to roughly 90%) by vanadium(III), with octahedral vanadium(IV) making up the remainder. In the titanomagnetite, as in hematite, both V^{3+} and V^{4+} replace Fe^{3+} in the octahedral site. The vanadium(IV) to vanadium(III) ratio was related to the oxygen fugacity of the magma during titanomagnetite crystallisation (Bordage et al., 2011).

As previously mentioned, slag residues from the steel industry often contain elevated vanadium levels. Blast furnace slags are dominated by vanadium(III), which is explained by the strongly reducing conditions in the blast furnace when the iron ore is melted (Larsson et al., 2015a). On the other hand, blast furnace oxygen slags, which are generated under more oxidizing conditions, are dominated by vanadium(IV) (Chaurand et al., 2006, 2007a) or by a mixture of vanadium(IV) and vanadate (Hobson et al., 2017). Aging, in the presence of atmospheric oxygen, was found to increase the V oxidation state (Chaurand et al., 2006, 2007a).

Most of the other investigated materials listed in Table 2 were dominated by vanadium(V), such as for example the red mud from the Ajka oil spill, Hungary, which was dominated by vanadate adsorbed to Fe and/or Al (hydr)oxides (Burke et al., 2013).

In conclusion, the use of XANES spectroscopy has led to a clearer understanding of the predominant V species, and their interconversions, in the environment. For oxic environments, such as the unsaturated zone of soils, vanadate(V) is usually the most stable oxidation state and in these, surface reactions with iron(III) and aluminium(III) compounds dominate the picture, although vanadate minerals such as volborthite may form in soils subject to extreme V contamination. Despite this, there are often substantial amounts of native V phases with lower oxidation states present in soils, as shown both for Swedish and for Thai soils (which are otherwise very different). However, these V phases are likely to have a very limited reactivity and may eventually be subject to weathering. A group of oxic soils with a different behaviour is the acid organic soils, where vanadyl(IV) complexes formed with organic matter are important. This will be further discussed in

section 5.2.

Concerning reducing environments, such as freshwater and marine sediments, much less is known about V speciation, although two recent XANES studies show that vanadium(III) and vanadium(IV) are the most stable under these conditions, which is in general accordance with the known redox behaviour of vanadium (see section 2). However, the exact phases involved are still unclear, particularly as concerns vanadium(III). It is known that V(III) may substitute for octahedral aluminium in clay minerals, but to what extent this process is really important in reduced sediments is still not known (Tribovillard et al., 2006).

4.3. Additional evidence on solid-phase vanadium speciation by use of other methods

Although less conclusive, sequential or selective extractions can provide additional evidence on V solubility and speciation. Table 3 summarizes a number of results, most of which are from relatively recent literature. A general impression is that V is recovered mainly from the less soluble fractions, which is in accordance with its strong sorption properties (e.g. Jeske and Gworek, 2012; Shaheen and Rinklebe, 2018), as detailed further in section 4.

Many past studies employed the sequential extraction methods of Tessier et al. (1979) or Rauret et al. (1999), or a version of these. These methods were developed primarily for metal cations. As discussed by Wenzel et al. (2001), for oxyanions such as arsenate(V) and vanadate (V) the interpretation of the results is not straightforward as desorption and subsequent resorption to other phases may occur in the extractants used in the different steps. The authors therefore developed a modified sequential extraction method based on desorption mediated by successively stronger competing ligands. This method should be better suited for estimating the relative solubility of V in soils where vanadate (V) dominates the V speciation. Studies using the method of Wenzel et al. (2001) include those of Tian et al. (2014) and Wright et al. (2014). A somewhat different approach was taken by Reijonen et al. (2016), who used the sequential extraction method of Zhang and Moore (1994), originally developed for selenium in wetlands, in an effort to determine the relative contributions of organically bound V and adsorbed vanadate(V) to the overall V speciation. After an initial extraction with 0.25 M KCl to recover "readily soluble V", specifically adsorbed vanadate(V) is desorbed with a 0.1 M *o*-phosphate solution. After that, an extraction with 0.1 M NaOH was assumed to represent organically bound V. When low additions of V were made to the two studied soil samples, between 30 and 68% of the V was found in the organically bound fraction, whereas only between 8 and 35% was assumed to be specifically adsorbed vanadate(V). However, a critical assumption is that 0.1 M *o*-phosphate desorbs all specifically adsorbed vanadate(V), and this was not examined.

Some authors (Tian et al., 2014, 2015; Xiao et al., 2015) combined results from sequential extractions with an estimate of to what extent vanadium was present as vanadium(IV) or vanadium(V) by use of the method of Mandiwana and Panichev (2004), according to which soil is boiled for 15 min in a solution containing 0.1 M Na_2CO_3 to recover vanadium(V). For example, Tian et al. (2015) spiked a soil with

Table 3
Summary of studies carrying out extractions to obtain information on the solubility and/or speciation of vanadium in environmental materials.

Materials studied	Method used	Results	Reference
One surface soil with high OM (1.7% OC) and one subsoil with low OM (0.3% OC)	Sequential extraction, modified from Zhang and Moore (1994), Chang and Jackson (1957)	Most added vanadium was recovered in a fraction assumed to represent organically bound V(IV), and a smaller proportion was vanadium(V) which, however, increased with increasing pH. The same trends were observed regardless of whether vanadium(IV) or vanadium(V) had been added	Reijonen et al. (2016)
Two A horizons of agricultural soils	Sequential extraction, modified from Tessier et al. (1979)	Vanadium was highest in the "organic" fraction	Poledniok and Buhl (2003)
One soil spiked with different V(V) concentrations	Sequential extraction, modified from Wenzel et al. (2001)	Most of the added V was probably pentavalent	Tian et al. (2014)
Chinese cabbage	Extraction of Na_2CO_3 to recover V(V), and ashing at 600 °C to recover V(IV) (Mandiwana and Panichev, 2004)	Predominance of V(IV)	Tian et al. (2014)
Five soils from an area polluted by vanadium mining and smelting operations	Sequential extraction, modified BCR extraction procedure	Most of the V was in the residual fraction, the highest % residual V (87%) was found in the smelting area	Cao et al. (2017)
As- and V-enriched Tertiary sediments from Melbourne, Australia	Separate extractions with $CaCl_2$, citrate-dithionite, oxalate, and sodium pyrophosphate	$CaCl_2$ extracted less than 0.5% of the V extracted by the other extractants, implying low solubility. Pyrophosphate extracted between 20 and 40% of pseudo-total V.	Mikkonen et al. (2019)
Wetland sediments after operation as constructed wetland	Sequential extraction	Most V was present in the acid-soluble fraction. After constructed wetland operation, more V was water-soluble apparently because of reducing conditions	Fox and Doner (2003)
Sediments disposed on land by dredging and overbank flooding	Sequential extraction using the modified BCR extraction procedure (Rauret et al., 1999)	Most V was in the residual fraction (usually > 50%), very low levels of V were in the acid-soluble fraction. Reducible V was larger than oxidizable V.	Cappuyns and Swennen (2014)
20 soil samples from mining areas that were placed in bioreactors	Sequential extraction, modified BCR extraction procedure	Microbial inoculation with added vanadate(V) decreased the fraction residual V	Hao et al. (2018)
Seven "rusty" soil profiles from Poland	Sequential extraction, modified from Tessier et al. (1979)	Only about 3% of V was present in the two most mobile fractions	Jeske and Gworek (2012)
13 soil profiles from Germany and Egypt	Sequential extraction using the modified BCR extraction procedure (Rauret et al., 1999)	Most V was in the residual fraction. Reducible V contributed more to V mobility than oxidizable V and was relatively higher in Egyptian soils	Shaheen and Rinklebe (2018)
One soil spiked with different V(V) concentrations	Extraction of Na_2CO_3 to recover V(V), and ashing at 600 °C to recover V(IV) (Mandiwana and Panichev, 2004)	V(IV) dominated V speciation in unamended soils, but addition of V(V) caused a larger proportion of V to be present as V(V)	Tian et al. (2015)
Six core samples from an aquifer	Sequential extraction, modified from Wenzel et al. (2001)	Most V was in strongly bound forms (HNO_3 or oxalate-ascorbate)	Wright et al. (2014)
19 soils polluted from coal mining	Sequential extraction (BCR) and Na_2CO_3 extraction to get V(V)	Most V was in the residual fraction. Between 9 and 49% of total V was V(V) in polluted soils, 11% in control soils	Xiao et al. (2015)

different vanadate(V) concentrations. After reaction, they found that the fraction if vanadium(V) in the soil increased with increasing initial dose vanadium(V) (see also Table 3). Although the V speciation results seem to be in reasonable agreement with the V K-edge XANES results reported in Table 2, Mandiwana and Panichev's method has, to the author's knowledge, not yet been validated with XANES or with any other direct speciation technique. Clearly such a method comparison would be very useful to properly evaluate the results obtained with Mandiwana and Panichev's method.

5. Vanadium binding to sorbents in soils and sediments - a quantitative analysis

5.1. Vanadium binding to iron and aluminium (hydr)oxides

In many soils the behaviour of vanadium is governed by vanadate (V) adsorption to iron(III) and aluminium(III) (hydr)oxides and silicates. High-surface-area iron(III) and aluminium(III) compounds such as ferrihydrite and allophane may be of particular importance in this regard (Larsson et al., 2017a).

Vanadate(V) adsorption to ferrihydrite has been studied by a relatively large number of authors (Leckie et al., 1984; Shieh and Duedall, 1988; Blackmore et al., 1996; Naeem et al., 2007; Brinza et al., 2008; Larsson et al., 2017b). Most of these studies show that vanadate(V) adsorption displays a maximum around pH 4, and then decreases above this value. However, vanadate(V) maintains strong adsorption up to at least a pH of 10, making it one of the most strongly adsorbing oxyanions on iron(III) (hydr)oxides. Two examples are shown in Fig. 10, in which the pH-dependent adsorption as observed in the systems of Shieh and Duedall (1988) and Blackmore et al. (1996) is displayed. In the latter study, the effect of competing *o*-phosphate anions was addressed and found to be small (Fig. 10); this is in agreement also with the study of Larsson et al. (2017b). The main reason why vanadate(V) adsorption drops below pH 4 is that under these conditions the speciation of vanadate(V) is dominated by the oxocation VO_2^+ (see section 2), which displays decreased adsorption as the pH value is decreased further. Similar vanadate(V) adsorption behaviour is observed also on goethite (Rietra, 2001; Peacock and Sherman, 2004).

So far, very limited quantitative information exists regarding vanadate(V) adsorption onto other sorbents such as aluminium (hydr) oxides and clay minerals. One exception is the study of Wehrli and Stumm (1989) who investigated vanadate(V) adsorption onto δ-Al_2O_3 and TiO_2 (anatase). Again a distinct adsorption maximum was observed, but it was located at a higher pH for both oxides compared to ferrihydrite, i.e. at pH between 5 and 6. It was also found that TiO_2 adsorbed vanadate(V) more efficiently at high pH than δ-Al_2O_3, despite the lower PZC (point-of zero charge) of the former. In another study, granular TiO_2 was found to an almost equally good sorbent for vanadate(V) as granular ferric hydroxide (Naeem et al., 2007). Wehrli and Stumm (1989) also studied the surface complexation of vanadyl(IV), i.e. VO^{2+}, to δ-Al_2O_3 and TiO_2 (anatase). Strong VO^{2+} sorption was observed down to pH 4 for both oxides studied, which is in line with VO^{2+} being a hard Lewis acid (harder, and more strongly adsorbing, than Pb^{2+}).

In principle, the adsorption patterns can be described in a consistent way by surface complexation models, which may also allow the prediction of vanadate(V) adsorption in the field. Dzombak and Morel (1990), who used the so-called Generalized Two Layer Model (GTLM), were the first to present a consistent database of surface complexation reactions for ferrihydrite. This model, also frequently referred to as the Diffuse Layer Model (DLM), has a simplified description of the solid-solution interface and only considers monodentate complexes, despite the fact that bidentate complexes predominate for many cations and oxyanions including vanadate(V). Dzombak and Morel (1990) used a number of data sets (Honeyman, 1984; Leckie et al., 1984), in which relatively low V/Fe ratios were used throughout, leading to very strong V adsorption below pH 10. As a consequence, the model for vanadate (V) was not fully parameterized. Wällstedt et al. (2010) updated the GLTM surface complexation constants using the data set of Blackmore et al. (1996; see Fig. 10), who studied also higher V/Fe ratios, permitting optimisation of constants for the surface complexes formed at lower pH. In the revised GLTM of Wällstedt et al. (2010), the GLTM surface complexation reactions for vanadate(V) are defined for three monodentate complexes M1, M2, and M3 as follows:

$$\text{M1. } \equiv\text{FeOH} + \text{HVO}_4^{2-} + 2\text{H}^+ \leftrightarrow \equiv\text{FeH}_2\text{VO}_4 + \text{H}_2\text{O} \qquad \log K_{M1} = 22.16 \quad (1)$$

$$\text{M2. } \equiv\text{FeOH} + \text{HVO}_4^{2-} + \text{H}^+ \leftrightarrow \equiv\text{FeHVO}_4^- + \text{H}_2\text{O} \qquad \log K_{M2} = 16.2 \quad (2)$$

$$\text{M3. } \equiv\text{FeOH} + \text{HVO}_4^{2-} + \text{H}^+ \leftrightarrow \equiv\text{FeHVO}_4^{2-} + \text{H}_2\text{O} \qquad \log K_{M3} = 9.0 \quad (3)$$

The equilibrium constants (*K*) contain an electrostatic correction term specific for the GTLM (c.f. Dzombak and Morel, 1990).

In their study on vanadate(V) sorption on ferrihydrite, Larsson et al. (2017b) instead used the CD-MUSIC model of Hiemstra and van Riemsdijk (1996), parameterized for ferrihydrite by Tiberg et al. (2013). The CD-MUSIC model has a more sophisticated description of

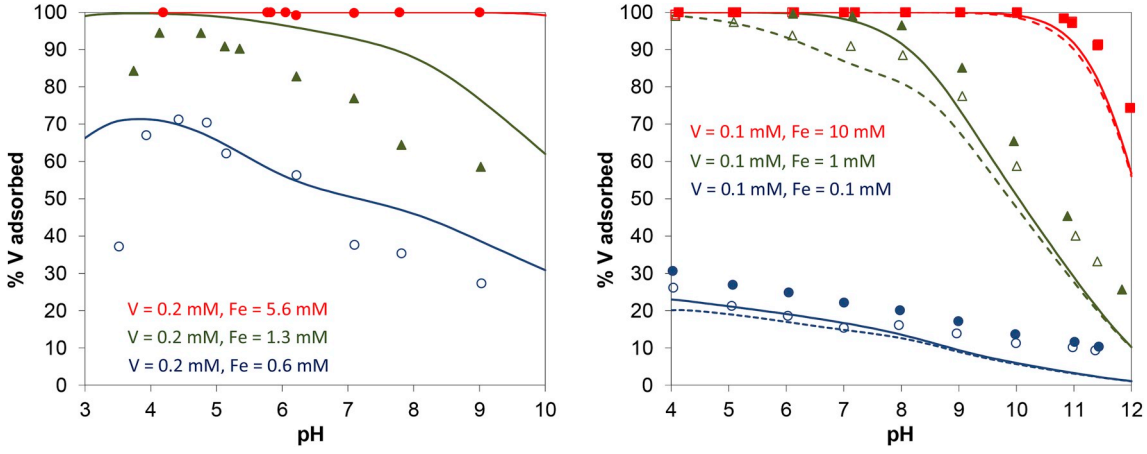

Fig. 10. Vanadate(V) adsorption to ferrihydrite as a function of pH. Left: Points are observed data of Shieh and Duedall (1988) with artificial seawater (I = 0.725 mol L^{-1}) as background. Right: Points are observed data of Blackmore et al. (1996) in a 0.01 mol L^{-1} $NaNO_3$ background. Empty symbols represent samples to which 0.1 mM *o*-phosphate had been added, whereas filled symbols are systems without *o*-phosphate. The lines represent the model fit using the CD-MUSIC model optimised for the data of Larsson et al. (2017b).

the solid-solution interface and allows consideration of bidentate coordination as constrained from spectroscopic results (c.f. section 4). The optimised model contained three bidentate complexes B1, B2 and B3 as follows:

$$\text{B1. } 2 \equiv \text{FeOH}^{0.5-} + \text{H}^+ + \text{HVO}_4^{2-} \leftrightarrow \ (\equiv\text{FeO})_2\text{VO}_2^{2-} + 2\text{H}_2\text{O} \qquad \log K_{B1} = 16.39 \tag{4}$$

$$\text{B2. } 2 \equiv \text{FeOH}^{0.5-} + 2\text{H}^+ + \text{HVO}_4^{2-} \leftrightarrow \ (\equiv\text{FeO})_2\text{VOOH}^- + 2\text{H}_2\text{O} \qquad \log K_{B2} = 23.20 \tag{5}$$

$$\text{B3. } 2 \equiv \text{FeOH}^{0.5-} + 3\text{H}^+ + \text{HVO}_4^{2-} \leftrightarrow \ (\equiv\text{FeO})_2\text{V(OH)}_2 + 2\text{H}_2\text{O} \qquad \log K_{B3} = 27.44 \tag{6}$$

Again the surface complexation constants contain electrostatic interaction factors, where the so called CD values, characteristic for the CD-MUSIC model, were optimised using PEST (Doherty, 2010), for more details see Larsson et al. (2017b). The most protonated complex, $(\equiv\text{FeO})_2\text{V(OH)}_2$, should very probably be understood as a complex involving the oxocation VO_2^+ (c.f. Peacock and Sherman, 2004). The model was applied in a fully predictive mode to the two previously mentioned data sets of Shieh and Duedall (1988) and Blackmore et al. (1996). While the model overpredicted vanadate(V) adsorption for the data of Shieh and Duedall (1988) it underpredicted the binding slightly for the data set of Blackmore et al. (1996). This can probably be explained by different procedures for ferrihydrite synthesis and ageing, as well as different reaction times in the experiment. For the data sets of Leckie et al. (1984) and Honeyman (1984), the model overpredicted vanadate(V) adsorption considerably (data not shown). However, in the two latter studies no effort was made to exclude CO_2 from the systems, and as most of the adsorption data were collected in the pH range from 8 to 11, competitive CO_3 adsorption may have influenced the result to an unknown extent, making it difficult to properly evaluate the model performance.

In Fig. 11 the model-predicted adsorption edges of different oxyanions on ferrihydrite are compared. Vanadate(V) is adsorbed most strongly of all the considered oxyanions, particularly at high pH. Although the presence of competing *o*-phosphate affects the adsorption of all oxyanions, the effect is smaller (but still clearly seen) for vanadate (V). These results suggest that the presence of iron (hydr)oxides in soils is of fundamental importance for the solubility (and bioavailability) of vanadium in the environment.

Also Peacock and Sherman (2004) optimised surface complexation models (Triple layer model, TLM, and DLM) to fit their vanadate(V) adsorption data on goethite. In this case, a combination of two bidentate complexes (analogous to B2 and B3 above) provided an acceptable fit to the data. Further, Rietra (2001) also reported one vanadate(V) adsorption data set for goethite, with data in the pH range from 8 to 10. In this case a CD-MUSIC model with one bidentate complex (B1) was sufficient to replicate the data.

Because of its ability to consider the actual surface coordination of vanadate(V), the CD-MUSIC model should be the preferred choice for the modelling of vanadate(V) adsorption to iron(III) (hydr)oxides. However, the GTLM/DLM is still often used in many publications, not least because it is still more widely spread and better known in the research community.

5.2. Vanadium binding to natural organic matter

Vanadyl(IV), VO^{2+}, forms strong complexes with natural organic matter. Szalay and Szilagyi (1967) were the first to observe that vanadate(V) added to humic acid was bound to a significant extent. They speculated that vanadate(V) had been reduced to vanadyl(IV), which was then complexed. Goodman and Cheshire (1975) proved that this was correct, and use of electron paramagnetic resonance (EPR) spectroscopy suggested vanadyl(IV) to be complexed predominantly by oxygen donor groups. Later, Templeton and Chasteen (1980) combined results from EPR with gel filtration experiments to show that the vanadyl(IV) was complexed by carboxylate and phenolate groups, and they also provided quantitative data for vanadyl(IV) binding onto fulvic acid, which was later used as a basis for estimating vanadyl(IV) binding in organic complexation models (Tipping, 1998; Milne et al., 2003). In the most recent version of WHAM, vanadyl(IV) binding is assumed to occur in mono-bi-, and tridentate coordination (Tipping et al., 2011), whereas the NICA-Donnan model assumes VO^{2+} to bind to two populations of sites that can be understood and low-affinity carboxylate and high-affinity phenolate, respectively (Kinniburgh et al., 1999).

Data on vanadyl(IV) binding onto solid-phase soil organic matter were provided by Gustafsson et al. (2007), who studied the effect of iron(III) on trace metal binding in a mor layer from a Spodosol. These data provided a basis for a database of vanadyl(IV) binding onto soil humic substances, used for the Stockholm Humic Model (SHM; Gustafsson, 2001). In this model, vanadyl(IV) binding is described by a combination of mono- and bidentate complexes, with the latter dominating under most conditions (c.f. Gustafsson et al., 2007). In Fig. 12, the simulated pH-dependent binding of VO^{2+} and other cations onto an organic soil is shown in the absence and presence of competing Fe^{3+} and Al^{3+}. As shown in the figure, the binding strength of VO^{2+} is comparable to those of Pb^{2+} and Cu^{2+}, and influenced significantly by competition from Fe^{3+} and Al^{3+}, although somewhat less so than for Pb^{2+} and Cu^{2+}.

Also vanadium(V) is known to form complexes with a wide range of organic molecules (Table S3 has examples of such reactions), although their complexation constants usually imply a weaker association than

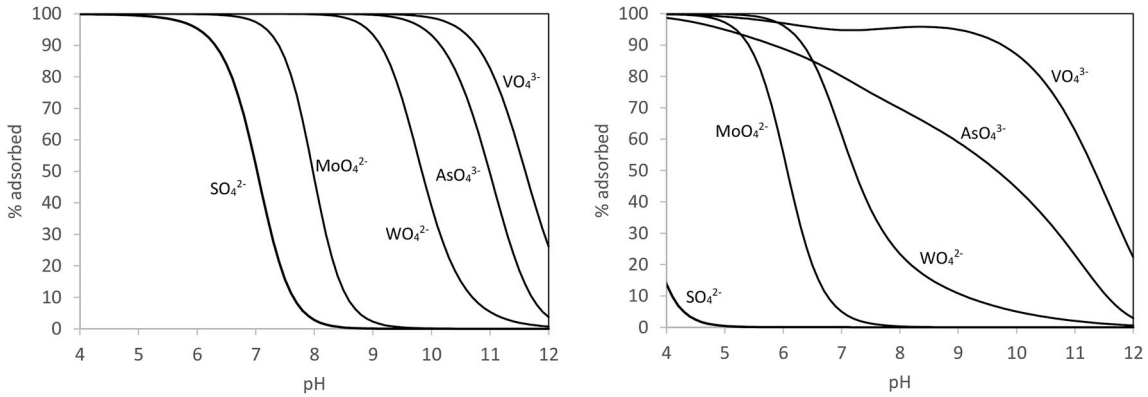

Fig. 11. Predicted adsorption of oxyanions to ferrihydrite as a function of pH (I = 0.01 M $NaNO_3$, ferrihydrite concentration = 0.3 g L^{-1}, total concentration of oxyanions = 1 μmol L^{-1} each) Left: no other competing ions present. Right: presence of 0.6 mmol L^{-1} *o*-phosphate. The lines are model fits using the CD-MUSIC model of Tiberg et al. (2013), as optimised for the vanadium data of Larsson et al. (2017b).

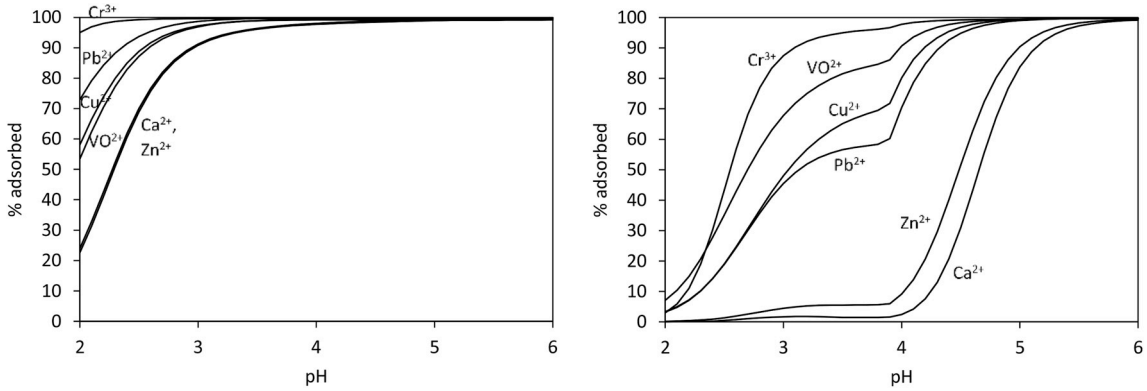

Fig. 12. Predicted adsorption of cations as a function of pH for a suspended organic soil containing 0.2 g L^{-1} fulvic acid and 0.6 g L^{-1} humic acid in the solid phase (I = 0.01 mol L^{-1} $NaNO_3$, DOC = 5 mg L^{-1}, total concentration of cations = 10 μmol L^{-1} each). Left: no other competing ions present. Right: presence of iron(III) governed by equilibrium with ferrihydrite (log $^*K_s$ = 2.69) and of 3 mM aluminium(III) that precipitates as $Al(OH)_3$(s) (log $^*K_s$ = 8.29) if saturation is reached. The lines are model fits using the Stockholm Humic Model of Gustafsson (2001), with VO^{2+} binding parameters of Gustafsson et al. (2007).

the corresponding vanadyl(IV) complexes. Still, in oxic soils at high Eh vanadium(V)-organic complexes could be expected to be more stable. As already mentioned, however, the reduction of vanadium(V) to vanadyl(IV) in systems with high concentrations of organic matter has frequently been observed, also under oxic conditions (Templeton and Chasteen, 1980; Lu et al., 1998; Larsson et al., 2015b). This is ascribed to the reducing ability of fulvic and humic acids (Lu et al., 1998) and may involve a hydroquinone group, which is oxidized to quinone; this reduction mechanism is efficient below pH 6. According to Lu et al. (1998), vanadium(V)-organic complexes may be more stable at high Eh in combination with near-neutral to alkaline pH conditions, but data are lacking, and there are no vanadium(V) binding parameters suggested for fulvic and humic acid.

5.3. Vanadium binding to soils – data and modelling

The number of published studies in which vanadium sorption to soils was studied is rather scarce. In an early study, Mikkonen and Tummavuori (1994) studied vanadate(V) sorption as a function of pH. The total addition was either 1 or 10 mmol V kg^{-1} soil, the shaking time was 72 h, and three Finnish mineral soil samples were studied in the pH range from 2.3 to 7.5. For all three soils and for both initial V concentrations the maximum V adsorption was observed at around pH 4 at which point between 70 and 80% of the added V was adsorbed.

So far there have been very few attempts to use surface complexation models or organic complexation models (described in previous sections) to predict vanadium mobility in soils. An exception is the study of Dijkstra et al. (2009) who applied a multisurface geochemical model to predict metal solubility in pH-static leaching tests for eight contaminated soils. For vanadium they used generic vanadyl(IV) binding parameters of the NICA-Donnan model for natural organic matter (Milne et al., 2003), and for vanadate(V) adsorption to ferrihydrite they used the GTLM of Dzombak and Morel, with surface complexation constants optimized for the data sets of Honeyman (1984) and Leckie et al. (1984). However, the RMSE of the model fit for V was around 1.2, poorest of all metals investigated. The model underestimated the V solubility at high pH, leading the authors to speculate that V was primarily present as vanadyl(IV) and not oxidized during the test. This assumption led to much improved model performance (Dijkstra et al., 2009).

Gäbler et al. (2009) carried out adsorption experiments with vanadate(V) for 30 German soils. In this case the added V concentration varied between 0.0005 and 0.5 mmol V kg^{-1} soil in a $Ca(NO_3)_2$ background. They were able to produce a large data set, which was used to derive Freundlich models for four groups of soils. These models can be used as first-hand approximations when no other data are available. The Freundlich equation can be written as:

$$Q = K_F \times c^m \quad (7)$$

where Q is the amount adsorbed V (expressed in μg V kg^{-1}), c is the dissolved V concentration (μg V L^{-1}), whereas K_F and m are fitted coefficients. For sandy soils, the optimised values for log K_F and m were found to be 2.55 and 0.59, respectively. The coefficient values for topsoils were 2.89 and 0.72, for subsoils with pH < 5.5 4.29 and 0.52, and for subsoils with pH > 5.5 3.41 and 0.57, respectively.

Larsson et al. (2017a) collected adsorption data for 26 European (mostly Swedish) soils. The added V concentration ranged from 0 to 4.5 mmol V kg^{-1}, and for 7 of the soils they also investigated the pH dependence of V binding, after an addition of 0.75 mmol V kg^{-1}. To fit the data, the authors used an extended Freundlich equation of the following form:

$$Q = K_F \times (c \times \{H^+\}^\eta)^m \quad (8)$$

where Q, K_F, m and c have the same meaning as in Equation (7), whereas η is an additional coefficient expressing the pH-dependence of vanadium sorption. Good fits were obtained for the investigated soils, but in contrast to the study of Gäbler et al. (2009) no effort was made to derive generalised coefficient values.

Both Gäbler et al. (2009) and Larsson et al. (2017a) showed that the content of iron(III) and aluminium(III) (hydr)oxides were important determinants for V sorption. Additional evidence from pH-dependent vanadate(V) sorption for seven soils and XANES studies for three soils (Table 2) led Larsson et al. (2017a) to conclude that vanadate(V) was very probably the predominant V oxidation state in all mineral soils studied, with the possible exception of one acid soil that had a relatively high organic matter content.

6. Environmental geochemistry of vanadium – additional evidence from the field

6.1. Vanadium transport through soils and aquifers

Martin and Kaplan (1998) investigated the movement of applied vanadyl(IV) in a Coastal Plain soil during 30 months, and the uptake of V to bush bean (*Phaseolorus vulgaris*) plants. After the experiment, less than 3% of the V had migrated below 7.5 cm depth, which showed that the V was strongly sorbed. Further, the extractability of the V decreased over the experimental period until 18 months, showing that the bioavailability of V gradually decreased during this period. The V uptake was consistent with this observation. The authors hypothesized that reactions with iron(III) and aluminium(III) (hydr)oxides limited the V bioavailability in this soil.

Telfeyan et al. (2015) studied V geochemistry along groundwater paths in two aquifers in the US, the Oasis valley and Carrizo sand aquifers. The groundwaters and aquifer sediments were thoroughly characterised and the total V concentration was measured in both media. Geochemical modelling was used to predict V speciation. In the Oasis valley aquifer, which was relatively alkaline and oxic, the average dissolved V concentration was 2.2 mg V L^{-1}, it was observed that the V concentrations increased along the flow path, probably because of increased supply from weathering. In the Carrizo Sand aquifer, which was much lower in dissolved V (0.023 mg V L^{-1}), and more reducing, the V concentrations decreased in the upper part, and then stayed more or less constant along the rest of the flow path. The authors concluded that vanadyl(IV) probably dominated in the Carrizo aquifer, and as the DOC concentrations were low, vanadyl(IV) instead was strongly sorbed in the aquifer material. In the Carrizo Sand aquifer, vanadate(V) predominated. In another study focusing on the seasonal cycling of vanadium in a freshwater deltaic marsh, Telfeyan et al. (2018) noted that dissolved V increased during late autumn and winter, possibly because of the decreased redox potential leading to reductive dissolution of Fe oxides containing adsorbed vanadate(V). However, there was no covariation between dissolved Fe and V, making it likely that other mechanisms were involved. Possibly vanadate(V) reduction to vanadyl(IV) and the association of the latter with dissolved organic matter were important mechanisms in this respect.

6.2. Influence of redox conditions on vanadium mobility

As the redox conditions are of fundamental importance for V geochemistry, it is of interest to study the dynamics of dissolved V when the redox conditions change quickly, e.g. after flooding. Amrhein et al. (1993) performed a laboratory incubation study with saline soils and sediments from San Joaquín valley, California, They observed that dissolved V increased after flooding, apparently due to release of adsorbed V after the reductive dissolution of iron (hydr)oxides and after reduction of vanadate(V) to vanadyl(IV). Similar results were obtained for floodplain soils from the area of Cologne, Germany (Frohne et al., 2015). In this case there was a highly significant inverse relationship between dissolved V and the redox potential (Eh) ($R^2 = 0.61$, $p < 0.0001$). A contributing factor to the strong relationship may have been high concentrations of DOC in this experiment, which caused a high solubility of organically complexed vanadyl(IV). In a column experiment where V-contaminated soil from China was leached with simulated acid rain the dissolved vanadium concentrations increased with time to reach a maximum of 71.3 μg V L^{-1} (Xiao et al., 2017). Again this was attributed to reductive dissolution of iron (hydr)oxides and the subsequent release of vanadium. However, for floodplain soils from the Nile delta, for which similar studies were carried out, there was no consistent trend for dissolved V with changes in Eh (Shaheen et al., 2014).

7. Conclusions

7.1. Processes governing V geochemistry and ecotoxicity

The biogeochemical cycle of vanadium has a strong contribution from human activities. The use of vanadium may increase further in the future due to the increased exploration of heavy petroleum resources, an increased demand of high-grade steel, and to the increased use of vanadium redox-flow batteries. Despite this, there is little evidence for widespread vanadium contamination of soils with the exception of areas near vanadium mines, coal mines, and oilfields. In Europe, most data suggest that the anthropogenic deposition of V has in fact decreased in recent times, probably due to reduced oil combustion and improved emission control.

The dissolved concentration of V is generally low, i.e. < 1 μg V L^{-1} in many waters that drain areas dominated by silicate rocks. In these areas dissolved V is strongly correlated with Si, showing that most of the V has been weathered. The mean dissolved V in the oceans is only marginally higher, i.e. at 1.8 μg V L^{-1}. However, the freshwaters of some areas with volcanic and sedimentary rocks are much higher in V and may in a few instances pose a health problem, e.g. in southern Italy.

The geochemistry of vanadium is rather complex, with three oxidation states (+III, +IV and +V) that may occur under natural conditions. In waters, dissolved vanadium normally consists of vanadyl(IV) and vanadate(V), with the latter dominating under oxic and relatively high-pH conditions, whereas the former occurs in reducing environments and at low-pH conditions particularly when dissolved organic matter is high. In soils, the solid-phase V is generally composed of a mixture of V strongly bound in primary minerals and of surface-bound V species. The former appears to be dominated by octahedrally coordinated vanadium(IV), whereas the surface-bound V often consists of vanadate(V) adsorbed to iron(III) and aluminium (hydr)oxides. Vanadate(V) adsorbs more strongly to iron (hydr)oxides than *o*-phosphate, and the surface complex is a bidentate complex. Organically complexed vanadyl(IV) may also be an important surface-bound V phase, particularly in acid organic soils where it may dominate V speciation. Vanadium(III) may be formed in the presence of sulphide, and has been identified as an important V phase in reduced sediments and in black shales. The dynamics of vanadium in the environment is strongly dependent on the redox conditions. Quick changes, i.e. due to flooding, may cause substantial increases or decreases of dissolved vanadium, but the effects are not the same everywhere.

Vanadium is an essential element for a few organisms. For example, it is present in V nitrogenase, which is used for N fixation particularly in boreal ecosystems. Vanadium haloperoxidases is another important group of biomolecules that mediate the oxidation of halides. However, at high concentrations of V, toxic effects may result. Most organisms in soils and waters show toxic effects in the mg L^{-1} range, but certain bacteria and algae may be affected at lower concentrations. Phosphate has been identified as an important determinant for V toxicity, and P-deficient systems show stronger V toxicity effects. In soils, the toxic response appears to be related to the dissolved V concentration and not to the solid-phase V concentration.

The methods to study vanadium geochemistry include X-ray absorption spectroscopy, which is the preferred method for solid-phase speciation, and various separation or spectrophotometric methods for the direct speciation of V in water. Stable isotope analysis using $^{51}V/^{50}V$ isotope ratios is a rapidly emerging research tool that has only begun to be used in low-temperature environments. Models for vanadium sorption to natural sorbents are available for ferrihydrite and natural organic matter, but so far little used for predicting vanadium mobility in the environment. The use of simpler empirical approaches (i.e. Freundlich models) appears to be a promising alternative.

7.2. Knowledge gaps

Overall the knowledge about vanadium geochemistry in the biogeosphere is relatively limited, when compared to elements such as copper, lead, cadmium and arsenic, which traditionally has been seen as high-priority pollutants. However, as vanadium receives more and more attention due to its widespread and increased use in society, it will be necessary to fill a number of knowledge gaps. Some that were identified during the course of writing this review include the following:

- *Thermodynamic data for vanadium(III).* The most reduced form of vanadium, vanadium(III), is also the form that is the least well researched as concerns its thermodynamics. For example, the

vanadium(III) hydrolysis constants appear uncertain. As these greatly affect the stability field of vanadium(III) versus vanadium (IV) and vanadium(V), more research is needed to constrain the hydrolysis constants further. In addition, the extent of vanadium(III) complexation to e.g. natural organic matter is yet to be determined. This process could be important for the understanding of vanadium geochemistry under strongly reducing (euxinic) conditions.

- *Vanadium speciation under reducing conditions, and on the microscale.* The first papers that reported V K-edge XANES data for reduced sediments were published in 2018 (Bennett et al., 2018; Nedrich et al., 2018). Still, we have very little information on the solid-phase V speciation in freshwater and marine sediments. Similarly, there is practically no information on the V speciation in black shales, despite the fact that these are often high in vanadium and may be an important future source of vanadium-containing ore. For both these types of environments it is not known, for example, how quickly and how efficiently V^{3+} is sorbed and incorporated into octahedral sites of oxides and clay minerals, and to what extent organic complexation may be an important solubility control. Moreover, most studies using XANES spectroscopy so far has used bulk V K-edge XANES spectroscopy to quantify speciation. The complementary use of spatially resolved techniques (e.g. synchrotron-XRF and μ-XANES) can, however, provide additional important insights into the geochemistry of V, as has been demonstrated e.g. by Terzano et al. (2007) and by Nesbitt and Lindsay (2017).
- *Ecotoxicity of vanadium, particularly the effect of phosphorus.* Ecotoxic effects appear in the mg L^{-1} range for many organisms, which is higher than the dissolved V concentration commonly encountered in waters. However, some studies report toxic effects on algae in the low μg L^{-1} range under P-deficient conditions (Lee et al., 1979; Nalewajko et al., 1995a, 1995b). When the results from such tests are included when deriving guidelines with species sensitivity distributions, very low values result, near background values of dissolved V (Smit, 2012). When they are excluded, much higher values are calculated, i.e. HC5 values of around 50 μg L^{-1} (Schiffer and Liber, 2017b). Similarly, the effect on plants strongly depends on the fertilization level (Smith et al., 2013). Thus, considerable uncertainty exists on how the results from toxicity tests with vanadium should be interpreted, in what way interacting *o*-phosphate affects the environmental risk, and how this interaction can be accounted for in risk assessments. There is urgent need for research that addresses these questions. Moreover, vanadium speciation is very probably an important aspect to consider for assessments of toxicity. There is a lack of studies that combine exotoxic effect studies with determination of the aqueous and solid-phase speciation of vanadium.
- *Sorption modelling of vanadium, and link to toxicity.* So far relatively few researchers have tested and/or developed models to predict the sorption/solubility of vanadium in soils. Although the efforts of Gäbler et al. (2009) and Larsson et al. (2017a) are promising, additional data sets are needed, and models (including multisurface models) need to be tested. Future research may include the development of models to predict possible V toxicity effects in soil through the biotic ligand model (di Toro et al., 2001) or by a similar approach. Because toxicity effects are primarily related to the soil solution concentration of V, it follows that it will be important to use a reliable model to account for the sorption of V to soil surfaces.
- *Dynamics of redox processes.* As vanadium is a redox-sensitive element, accurate understanding of its behaviour requires detailed knowledge on the different processes that contribute to the vanadium redox conversions and the changes in solubility and bioavailability that may result. The role of microorganisms, and the genera of bacteria that carry out these conversions, are beginning to be unravelled, but much more remains to be known. For example, this knowledge is important when devising efficient bioremediation methods for vanadium-contaminated environments.

Acknowledgements

First of all I thank Maja Larsson, our previous PhD student, who authored six papers during her PhD studies, all of which are mentioned in this review. I also thank my other “vanadium collaborators” from previous research projects, Stijn Baken, Erik Smolders, Golshid Hadialhejazi, Francesco Cubadda, Andrea Raggi, Marilena D'Amato, Ingrid Öborn, Dan Berggren Kleja, Ingrid Öborn, Ingmar Persson, Carin Sjöstedt, and Lars Johnsson. Torbjörn Carlsson and Jeanette Stemne at Merox are the ones who introduced us into the vanadium world and are hereby thankfully acknowledged. Rolf Lindblom at LKAB is thanked for stimulating discussions. The EXAFS results for vanadium sorbed on amorphous Al hydroxide were collected at beamline I811, MAX-Lab synchrotron radiation source, Lund University, Sweden. Funding for the beamline I811 project was kindly provided by The Swedish Research Council and The Knut och Alice Wallenbergs Stiftelse.

Appendix A. Supplementary data

Supplementary data to this article can be found online at https://doi.org/10.1016/j.apgeochem.2018.12.027.

References

Allison, J.D., Brown, D.S., Novo-Gradac, K.J., 1991. MINTEQA2/PRODEFA2. A geochemical assessment model for environmental systems. U.S. EPA, Athens, GA 30613, USA EPA/600/3-91/021.

Amrhein, C., Mosher, P.A., Brown, A.D., 1993. The effects of redox on Mo, U, B, V, and As solubility in evaporation pond soils. Soil Sci. 155, 249–255. https://doi.org/10.1097/00010694-199304000-00003.

Antipov, A.N., Lyalikova, N.N., Khijniak, T.V., L'vov, N.P., 1998. Molybdenum-free nitrate reductases from vanadate-reducing bacteria. FEBS Lett. 451, 257–260. https://doi.org/10.1016/S0014-5793(98)01510-5.

Arena, G., Copat, C., Dimartino, A., Grasso, A., Fallico, R., Sciacca, S., Fiore, M., Ferrante, M., 2015. Determination of total vanadium and vanadium(V) in groundwater from Mt. Etna and estimate of daily intake of vanadium(V) through drinking water. J. Water Health 13 (2), 522–530. https://doi.org/10.2166/wh.2014.209.

Auger, Y., Bodineau, L., Leclercq, S., Wartel, M., 1999. Some aspects of vanadium and chromium chemistry in the English Channel. Cont. Shelf Res. 19, 2003–2018. https://doi.org/10.1016/S0278-4343(99)00050-3.

Aureli, F., Ciardullo, S., Pagano, M., Raggi, A., Cubadda, F., 2008. Speciation of vanadium (IV) and (V) in mineral water by anion exchange liquid chromatography-inductively coupled plasma mass spectrometry after EDTA complexation. J. Anal. At. Spectrom. 23, 1009–1016. https://doi.org/10.1039/B805234B.

Baken, S., Larsson, M.A., Gustafsson, J.P., 2012. Soil Sci. 63, 839–847. https://doi.org/10.1111/j.1365-2389.2012.01491.x.

Balan, E., De Villiers, J.P.R., Eeckhout, S.G., Glatzel, P., Toplis, M.J., Fritsch, E., Allard, T., Galoisy, L., Calas, G., 2006. The oxidation state of vanadium in titanomagnetite from layered basic intrusions. Am. Mineral. 91, 953–956. https://doi.org/10.2138/am.2006.2192.

Bauer, S., Blomqvist, S., Ingri, J., 2017. Distribution of dissolved and particulate molybdenum, vanadium, and tungsten in the Baltic Sea. Mar. Chem. 196, 135–147. https://doi.org/10.1016/j.marchem.2017.08.010.

Bayer, E., Koch, E., Anderegg, G., 1987. Amavadin, an example for selective binding of vanadium in nature: studies of its complexation chemistry and a new structural proposal. Angew. Chem. Int. Ed. 26, 545–546. https://doi.org/10.1002/anie.198705451.

Bennett, W.W., Lombi, E., Burton, E.D., Johnston, S.G., Kappen, P., Howard, D.L., Canfield, D.E., 2018. Synchrotron X-ray spectroscopy for investigating vanadium speciation in marine sediment. Limitations and opportunities. J. Anal. At. Spectrom. 33, 1689–1699. https://doi.org/10.1039/C8JA00231B.

Benzi, F., Giuli, G., Della Longa, S., Paris, E., 2016. Vanadium K-edge XANES in vanadium-bearing model compounds: a full multiple scattering study. J. Synchrotron Radiat. 23, 947–952. https://doi.org/10.1107/S1600577516008134.

Berry, R.E., Armstrong, E.M., Beddoes, R.L., Collison, D., Ertok, S.N., Helliwell, M., Garner, C.D., 1999. The structural characterization of amavadin. Angew. Chem. Int. Ed. 38, 795–797. https://doi.org/10.1002/(SICI)1521-3773(19990315)38:6%3C795::AID-ANIE795%3E3.0.CO;2-7.

Blackmore, D.P.T., Ellis, J., Riley, P.J., 1996. Treatment of a vanadium-containing effluent by adsorption/coprecipitation with iron oxyhydroxide. Water Res. 30, 2512–2516. https://doi.org/10.1016/0043-1354(96)00080-2.

Boechat, C.B., Eon, J.G., Rossi, A.M., Perez, C.A.D., San Gil, R.A.D., 2000. Structure of vanadate in calcium phosphate and vanadate apatite solid solutions. Phys. Chem. Chem. Phys. 2, 4225–4230. https://doi.org/10.1039/B004339G.

Bordage, A., Balan, E., de Villiers, J.P.R., Cromarty, R., Juhin, A., Carvallo, C., Calas, G., Sunder Raju, P.V., Glatzel, P., 2011. V oxidation state in Fe-Ti oxides by high-energy resolution fluorescence-detected X-ray absorption spectroscopy. Phys. Chem. Miner. 338, 449–458. https://doi.org/10.1007/s00269-011-0418-3.

Borg, H., 1984. Background levels of trace metals in Swedish freshwaters. Naturvårdsverket, PM 1817. Solna, Sweden.
Bredberg, K., Karlsson, H.T., Holst, O., 2004. Reduction of vanadium(V) with *Acidithiobacillus ferrooxidans* and *Acidithiobacillus thiooxidans*. Bioresour. Technol. 92, 93–96. https://doi.org/10.1016/j.biortech.2003.08.004.
Breit, G.N., Wanty, R.B., 1991. Vanadium accumulation in carbonaceous rocks: a review of geochemical controls during deposition and diagenesis. Chem. Geol. 91, 83–97. https://doi.org/10.1016/0009-2541(91)90083-4.
Brinza, L., Benning, L.G., Statham, P.J., 2008. Adsorption studies of Mo and V onto ferrihydrite. Miner. Mag. 72, 385–388. https://doi.org/10.1180/minmag.2008.072.1.385.
Bruyère, V.I.E., García Rodenas, L.A., Morando, P.J., Blesa, M.A., 2001. Reduction of vanadium(V) by oxalic acid in aqueous acid solutions. J. Chem. Soc. Dalton Trans. 2001, 3593–3597. https://doi.org/10.1039/B103320B.
Buglyó, P., Crans, D.C., Nagy, E.M., Lindo, R.L., Yang, L., Smee, J.J., Jin, W., Chi, L.-H., Godzala, M.E., Willsky, G.R., 2005. Aqueous chemistry of the vanadium(^{III}) (V^{III}) and the V^{III}-dipicolinate systems and the comparison of the state of three oxidation states of vanadium compounds on the diabetic hyperglycemia in rats. Inorg. Chem. 44, 5416–5427. https://doi.org/10.1021/ic048331q.
Burke, I.T., Mayes, W.M., Peacock, C.L., Brown, A.P., Jarvis, A.P., Gruiz, K., 2012. Speciation of arsenic, chromium, and vanadium in red mud samples from the Ajka spill site, Hungary. Environ. Sci. Technol. 46, 3085–3092. https://doi.org/10.1021/es3003475.
Burke, I.T., Peacock, C.L., Lockwood, C.L., Stewart, D.I., Mortimer, R.J.G., Ward, M.B., Renforth, P., Gruiz, K., Mayes, W.M., 2013. Behavior of aluminum, arsenic, and vanadium during the neutralization of red mud leachate by HCl, gypsum, or seawater. Environ. Sci. Technol. 47, 6527–6535. https://doi.org/10.1021/es4010834.
Cao, X., Diao, M., Zhang, B., Liu, H., Wang, S., Yang, M., 2017. Spatial distribution and microbial community responses in surface soil of Panzhihua mining and smelting area, China. Chemosphere 183, 9–17. https://doi.org/10.1016/j.chemosphere.2017.05.092.
Cappuyns, V., Slabbinck, E., 2012. Occurrence of vanadium in Belgian and European alluvial soils. Appl. Environ. Soil Sci. 979501. https://doi.org/10.1155/2012/979501.
Cappuyns, V., Swennen, R., 2014. Release of vanadium from oxidized sediments: insights from different extraction and leaching procedures. Environ. Sci. Pollut. Res. 21, 2272–2282. https://doi.org/10.1007/s11356-013-2149-0.
Carlson, C.L., Adriano, D.C., Sajwan, K.S., Abels, S.L., Thoma, D.P., Driver, D.T., 1991. Effects of selected trace metals on germinating seeds of six plant species. Water Air Soil Pollut. 59, 231–240. https://doi.org/10.1007/BF00211832.
Carpentier, W., Sandra, K., De Smet, I., Brigé, A., De Smet, L., Van Beeumen, J., 2003. Microbial reduction and precipitation of vanadium by *Shewanella oneidensis*. Appl. Environ. Microbiol. 69, 3636–3639. https://doi.org/10.1128%2FAEM.69.6.3636-3639.2003.
Caswell, L.R., 2003. Andrés del Río, Alexander von Humboldt, and the twice-discovered element. Bull. Hist. Chem. 28, 35–41.
Ceci, A., Rhee, Y.J., Kierans, M., Hillier, S., Pendlowski, H., Gray, N., Persiani, A.M., Gadd, G.M., 2015. Transformation of vanadinite [$Pb_5(VO_4)_3Cl$] by fungi. Environ. Microbiol. 17, 2018–2034. https://doi.org/10.1111/1462-2920.12612.
Chang, S.C., Jackson, M.L., 1957. Fractionation of soil phosphorus. Soil Sci. 84, 133–144.
Chaurand, P., Rose, J., Domas, J., Bottero, J.Y., 2006. Speciation of Cr and V within BOF steel slag reused in road constructions. J. Geochem. Explor. 88, 10–14. https://doi.org/10.1016/j.gexplo.2005.08.006.
Chaurand, P., Rose, J., Briois, V., Olivi, L., Hazemann, J.L., Proux, O., Domas, J., Bottero, J.Y., 2007a. Environmental impacts of steel slag reused in road construction: A crystallographic and molecular (XANES) approach. J. Hazard Mater. 139, 537–542. https://doi.org/10.1016/j.jhazmat.2006.02.060.
Chaurand, P., Rose, J., Briois, V., Salome, M., Proux, O., Nassif, V., Olivi, L., Susini, J., Hazemann, J.L., Bottero, J.Y., 2007b. New methodological approach for the vanadium K-edge X-ray absorption near-edge structure interpretation: Application to the speciation of vanadium in oxide phases from steel slag. J. Phys. Chem. B111, 5101–5110. https://doi.org/10.1021/jp063186i.
Chen, Z.L., Owens, G., 2008. Trends in speciation analysis of vanadium in environmental samples and biological fluids - A review. Anal. Chim. Acta 607, 1–14. https://doi.org/10.1016/j.aca.2007.11.013.
Chen, S., Zhang, S., Wang, T., Lei, Z., Zhu, M., Dai, X., Liu, F., Li, J., Yin, H., 2018. Structure and properties of vanadium-doped α-MnO_2 and enhanced Pb^{2+} adsorption phenol/photocatalytic degradation. Mater. Chem. Phys. 208, 258–267. https://doi.org/10.1016/j.matchemphys.2018.01.046.
Chermak, J.A., Schreiber, M.E., 2014. Mineralogy and trace element geochemistry of gas shales in the United States: Environmental implications. Int. J. Coal Geol. 126, 32–44. https://doi.org/10.1016/j.coal.2013.12.005.
Cloy, J.M., Farmer, J.G., Graham, M.C., MacKenzie, A.G., 2010. Scottish peat bog records of atmospheric vanadium deposition over the past 150 years: comparison with other records and emission trends. J. Environ. Monit. 13, 58–65. https://doi.org/10.1039/c0em00492h.
Cornelis, G., Johnson, C.A., Van Gerven, T., Vandecasteele, C., 2008. Leaching mechanisms of oxyanionic metalloid and metal species in alkaline solid wastes: a review. Appl. Geochem. 233, 955–976. https://doi.org/10.1016/j.apgeochem.2008.02.001.
Costa Pessoa, J., Garribba, E., Santos, M.F.A., Santos-Silva, T., 2015. Vanadium and proteins: uptake, transport, structure, activity and function. Coord. Chem. Rev. 301–302, 49–86. https://doi.org/10.1016/j.ccr.2015.03.016.
Crans, D.C., Smee, J.J., Gaidamauskas, E., Yang, L., 2004. The chemistry and biochemistry of vanadium and the biological activities exerted by vanadium compounds. Chem. Rev. 104, 849–902. https://doi.org/10.1021/cr020607t.
Cruywagen, J.J., 1999. Protonation, oligomerization, and condensation reactions of vanadate(V), molybdate(VI), and tungstate(VI). Adv. Inorg. Chem. 49, 127–182. https://doi.org/10.1016/S0898-8838(08)60270-6.
da Silva, J.A.L., da Silva, J.J.R.F., Pombeiro, A.J.L., 2013. Amavadin, a vanadium natural complex: its role and applications. Coord. Chem. Rev. 257, 2388–2400. https://doi.org/10.1016/j.ccr.2013.03.010.
Darnajoux, R., Constantin, J., Miadlikowska, J., Lutzoni, F., Bellenger, J.-P., 2014. Is vanadium a biometal for boreal cyanolichens? New Phytol. 202, 765–771. https://doi.org/10.1111/nph.12777.
Darnajoux, R., Zhang, X., McRose, D.L., Miadlikowska, J., Lutzoni, F., Kraepiel, A.M.L., Bellenger, J.-P., 2017. Biological nitrogen fixation by alternative nitrogenases in boreal cyanolichens: importance of molybdenum bioavailability and implications for current biological nitrogen fixation estimates. New Phytol. 213, 680–689. https://doi.org/10.1111/nph.14166.
De Vos, W., Tarviainen, T. (Eds.), 2006. Geochemical atlas of Europe. Part 2 – Interpretation of geochemical maps, additional tables, figures, maps, and related publications. Geological Survey of Finland, Espoo, Finland.
De Windt, L., Chaurand, P., Rose, J., 2011. Kinetics of steel slag leaching: batch tests and modelling. Waste Manag. 31, 225–235. https://doi.org/10.1016/j.wasman.2010.05.018.
Dechaine, G.P., Gray, M.R., 2010. Chemistry and association of vanadium compounds in heavy oil and bitumen, and implications for their selective removal. Energy Fuels 24, 2795–2808. https://doi.org/10.1021/ef100173j.
di Toro, D.M., Allen, H.E., Bergman, H.L., Meyer, J.S., Paquin, P.R., Santore, R.C., 2001. Biotic ligand model of the acute toxicity of metals. 1. Technical basis. Environ. Toxicol. Chem. 20, 2383–2396. https://doi.org/10.1002/etc.5620201034.
Dijkstra, J.J., Meeussen, J.C.L., Comans, R.N.J., 2009. Evaluation of a generic multisurface sorption model for inorganic soil contaminants. Environ. Sci. Technol. 43, 6196–6201. https://doi.org/10.1021/es900555g.
Dobrovolsky, V.V., 1994. Biogeochemistry of the world's land. CRC Press, Boca Raton, Florida.
Doherty, J., 2010. PEST, Model-independent parameter estimation, User Manual, fifth ed. Watermark Numerical Computing, Bethesda, MD., USA.
Duchesne, M.A., Nakano, J., Hu, Y.,, MacLennan, A., Bennett, J., Nakano, A., Hughes, R.W., 2018. Synchrotron-based X-ray absorption spectroscopy study of vanadium redox speciation during petroleum coke combustion and gasification. Fuel 227, 279–288. https://doi.org/10.1016/j.fuel.2018.04.104.
Dzombak, D.A., Morel, F.M.M., 1990. Surface complexation modeling. Wiley & Sons, New York.
Edwards, R., Lepp, N.W., Jones, K.C., 1995. Antimony and vanadium. In: Alloway, B.J. (Ed.), Heavy metals in soils, second ed. Blackie Academic & Professional, Glasgow, pp. 346–352.
Elvingson, K., Baro, A.G., Pettersson, L., 1996. Speciation of vanadium in bioinorganic systems: 2. An NMR, ESR, and potentiometric study of the aqueous H^+-vanadate-maltol system. Inorg. Chem. 35, 3388–3393. https://doi.org/10.1021/ic951195s.
Fox, P.M., Doner, H.E., 2003. Accumulation, release, and solubility of arsenic, molybdenum, and vanadium in wetland sediments. J. Environ. Qual. 32, 2428–2435. https://doi.org/10.2134/jeq2003.2428.
Frank, A., Madej, A., Galgan, V., Petersson, L.R., 1996. Vanadium poisoning of cattle with basic slag. Concentrations in tissues from poisoned animals and from a reference, slaughter-house material. Sci. Total Environ. 181, 73–92. https://doi.org/10.1016/0048-9697(95)04962-2.
Frank, P., Hodgson, K.O., Kustin, K., Robinson, W.E., 1998. Vanadium K-edge X-ray absorption spectroscopy reveals species differences within the same ascidian genera. J. Biol. Chem. 273, 24498–24503. https://doi.org/10.1074/jbc.273.38.24498.
Frank, P., Carlson, R.M.K., Carlson, E.J., Hodgson, K.O., 2003. The vanadium environment in blood cells of Ascidia ceratodes is divergent at all organismal levels: an XAS and EPR spectroscopic study. J. Inorg. Biochem. 94, 59–71. https://doi.org/10.1016/S0162-0134(02)00636-0.
Frank, P., Carlson, E.J., Carlson, R.M.K., Hedman, B., Hodgson, K.O., 2008. The uptake and fate of vanadyl ion in ascidian blood cells and a detailed hypothesis for the mechanism and location of biological vanadium reduction. A visible and X-ray absorption spectroscopic study. J. Inorg. Biochem. 102, 809–823. https://doi.org/10.1016/j.jinorgbio.2007.12.001.
Frank, P., Hedman, B., Hodgson, K.O., 2014. XAS spectroscopy, sulfur, and the brew within blood cells from Ascidia ceratodes. J. Inorg. Biochem. 131, 99–108. https://doi.org/10.1016/j.jinorgbio.2013.11.004.
Frohne, T., Diaz-Bone, R.A., Du Laing, G., Rinklebe, J., 2015. Impact of systematic change of redox potential on the leaching of Ba, Cr, Sr, and V from a riverine soil into water. J. Soils Sediments 15, 623–633. https://doi.org/10.1007/s11368-014-1036-8.
Gäbler, H.E., Gluh, K., Bahr, A., Utermann, J., 2009. Quantification of vanadium adsorption by German soils. J. Geochem. Explor. 103, 37–44. https://doi.org/10.1016/j.gexplo.2009.05.002.
Gamage, S.V., Hodge, V.F., Cizdziel, J.V., Lindley, K., 2010. Determination of vanadium (IV) and (V) in Southern Nevada groundwater by ion chromatography-inductively coupled plasma mass spectrometry. Open Chem. Biomed. Methods J. 3, 10–17. https://doi.org/10.2174/1875038901003010010.
Gao, Y., Casey, J.F., Bernardo, L.M., Yang, W., Bissada, K.K., 2017. Vanadium isotope composition of crude oil: effects of source, maturation and biodegradation. Geol. Soc. London Spec. Publ. 468, 83–103. https://doi.org/10.1144/SP468.2.
García-Jiménez, A., Trejo-Téllez, L.I., Guillén-Sánchez, D., Gómez-Merino, F.C., 2018. Vanadium stimulates pepper plant growth and flowering, increases concentrations of amino acids, sugars and chlorophylls, and modifies nutrient concentrations. PLoS One 13 (8), e0201908. https://doi.org/10.1371/journal.pone.0201908.
Gardner, C.B., Carey, A.E., Lyons, W.B., Goldsmith, S.T., McAdams, B.C., Trierweiler, A.M., 2017. Molybdenum, vanadium, and uranium weathering in small mountainous rivers and rivers draining high-standing islands. Geochem. Cosmochim. Acta 219,

22–43. https://doi.org/10.1016/j.gca.2017.09.012.
Gehring, A.U., Fry, I.V., Luster, J., Sposito, G., 1993. The chemical form of vanadium(IV) in kaolinite. Clay Clay Miner. 41, 662–667. https://doi.org/10.1346/CCMN.1993.0410604.
Gehring, A.U., Fry, I.V., Luster, J., Sposito, G., 1994. Vanadium in sepioloite: a redox indicator for an ancient closed brine system in the Madrid system, Central Spain. Geochem. Cosmochim. Acta 58, 3345–3351. https://doi.org/10.1016/0016-7037(94)90090-6.
George, G.N., Coyle, C.L., Hales, B.J., Cramer, S.P., 1988. X-ray absorption of *Azotobacter vinelandii* vanadium nitrogenase. J. Am. Chem. Soc. 110, 4057–4059. https://doi.org/10.1021/ja00220a066.
Gerke, T.L., Scheckel, K.G., Schock, M.R., 2009. Identification and distribution of vanadinite ($Pb_5(V^{5+}O_4)_3Cl$) in lead pipe corrosion by-products. Environ. Sci. Technol. 43, 4412–4418. https://doi.org/10.1021/es900501t.
Gerke, T.L., Scheckel, K.G., Maynard, J.B., 2010. Speciation and distribution of vanadium in drinking water iron pipe corrosion by-products. Sci. Total Environ. 408, 5845–5853. https://doi.org/10.1016/j.scitotenv.2010.08.036.
Gil, J., Alvarez, C.E., Martinez, M.C., Perez, N., 1995. Effect of vanadium on lettuce growth, cationic nutrition, and yield. J. Environ. Sci. Health A30 73–87. https://doi.org/10.1080/10934529509376186.
Goodman, B.A., Cheshire, M.V., 1975. The bonding of vanadium in complexes with humic acid: an electron paramagnetic resonance study. Geochem. Cosmochim. Acta 39, 1711–1713. https://doi.org/10.1016/0016-7037(75)90093-9.
Gräfe, M., Landers, M., Tappero, R., Austin, P., Gan, B., Grabsch, A., Klauber, C., 2011. Combined application of QEM-SEM and hard X-ray microscopy to determine mineralogical associations and chemical speciation of trace metals. J. Environ. Qual. 40, 767–783. https://doi.org/10.2134/jeq2010.0214.
Guagliardi, I., Cicchella, D., De Rosa, R., Ricca, N., Buttafuoco, G., 2018. Geochemical sources of vanadium in soils: evidences in a southern Italy area. J. Geochem. Explor. 184, 358–364. https://doi.org/10.1016/j.gexplo.2016.11.017.
Gustafsson, J.P., 2001. Modeling the acid-base properties and metal complexation of humic substances with the Stockholm Humic Model. J. Colloid Interface Sci. 244, 102–112. https://doi.org/10.1006/jcis.2001.7871.
Gustafsson, J.P., 2018. Visual MINTEQ ver. 3.1. https://vminteq.lwr.kth.se, Accessed date: 30 October 2018.
Gustafsson, J.P., Johnsson, L., 2004. Vanadin i svensk miljö – förekomst och toxicitet. TRITA-LWR report 3009. KTH Royal Institute of Technology, Stockholm, Sweden.
Gustafsson, J.P., Tiberg, C., 2015. Molybdenum binding to soil constituents in acid soils: an XAS and modelling study. Chem. Geol. 417, 279–288. https://doi.org/10.1016/j.chemgeo.2015.10.016.
Gustafsson, J.P., Persson, I., Kleja, D.B., van Schaik, J.W.J., 2007. Binding of iron(III) to organic soils: EXAFS spectroscopy and chemical equilibrium modeling. Environ. Sci. Technol. 41, 1232–1237. https://doi.org/10.1021/es0615730.
Hamada, T., 1998. High vanadium content in Mt. Fuji groundwater and its relevance to the ancient biosphere. In: Nriagu, J.O. (Ed.), Vanadium in the Environment. Part 1: Chemistry and biochemistry. Wiley & Sons, New York, pp. 97–123.
Hao, L., Zhang, B., Feng, C., Zhang, Z., Lei, Z., Shimizu, K., Cao, X., Liu, H., Liu, H., 2018. Microbial vanadium(V) reduction in groundwater with different soils from vanadium ore mining areas. Chemosphere 202, 272–279. https://doi.org/10.1016/j.chemosphere.2018.03.075.
Harmens, H., Norris, D.A., Koerber, G.R., Buse, A., Steinnes, E., Rühling, Å., 2007. Temporal trends in the concentration of arsenic, chromium, copper, iron, nickel, vanadium and zinc in mosses across Europe between 1990 and 2000. Atmos. Environ. 41, 6673–6687. https://doi.org/10.1016/j.atmosenv.2007.03.062.
Hernandez, H., Rodriguez, R., 2012. Geochemical evidence for the origin of vanadium in an urban environment. Environ. Monit. Assess. 184, 5327–5342. https://doi.org/10.1007/s10661-011-2343-9.
Hiemstra, T., 2013. Surface and mineral structure of ferrihydrite. Geochem. Cosmochim. Acta 105, 316–325. https://doi.org/10.1016/j.gca.2012.12.002.
Hiemstra, T., van Riemsdijk, W.H., 1996. A surface structural approach to ion adsorption: The charge distribution (CD) model. J. Colloid Interface Sci. 179, 488–508. https://doi.org/10.1006/jcis.1996.0242.
Ho, P., Lee, J.-M., Heller, M.I., Lam, P.J., Shiller, A.M., 2018. The distribution of dissolved and particulate Mo and V along the U.S. GEOTRACES East Pacific zonal transect (GP16): the roles of oxides and biogenic particles in their distributions in the oxygen deficient zone and the hydrothermal plume. Mar. Chem. 201, 242–255. https://doi.org/10.1016/j.marchem.2017.12.003.
Hobson, A.J., Stewart, D.I., Bray, A.W., Mortimer, R.J.G., Mayes, W.M., Rogerson, M., Burke, I.T., 2017. Mechanism of vanadium leaching during surface weathering of basic oxygen furnace steel slag blocks: a microfocus X-ray absorption spectroscopy and electron microscopy study. Environ. Sci. Technol. 51, 7823–7830. https://doi.org/10.1021/acs.est.7b00874.
Hobson, A.J., Stewart, D.I., Bray, A.W., Mortimer, R.J.G., Mayes, W.M., Riley, A.L., Rogerson, M., Burke, I.T., 2018. Behaviour and fate of vanadium during the aerobic neutralisation of hyperalkaline slag leachate. Sci. Total Environ. 643, 1191–1198. https://doi.org/10.1016/j.scitotenv.2018.06.272.
Honeyman, B.D., 1984. Cation and anion adsorption at the oxide/solution interface in systems containing binary mixtures of adsorbents: an investigation of the concept of adsorptive additivity. PhD thesis. Stanford University, Stanford, CA, USA.
Hope, B.K., 1994. A global biogeochemical budget for vanadium. Sci. Total Environ. 141, 1–10. https://doi.org/10.1016/0048-9697(94)90012-4.
Hope, B.K., 2008. A dynamic model for the global cycling of anthropogenic vanadium. Glob. Biogeochem. Cycles 22, GB4021. https://doi.org/10.1029/2008GB003283.
Huang, J.-W., Huang, F., Evans, L., Glasauer, S., 2015. Vanadium: global (bio)geochemistry. Chem. Geol. 417, 68–89. https://doi.org/10.1016/j.chemgeo.2015.09.019.
Huggins, F.E., Huffman, G.P., Robertson, J.D., 2000. Speciation of elements in NIST particulate matter SRMs 1648 and 1650. J. Hazard Mater. 74, 1–23. https://doi.org/10.1016/S0304-3894(99)00195-8.
Huijgen, W.J.J., Comans, R.N.J., 2006. Carbonation of steel slag for CO2 sequestration: leaching of products and mechanisms. Environ. Sci. Technol. 40, 2790–2796. https://doi.org/10.1021/es052534b.
Jensen-Fontaine, M., Norwood, W.P., Brown, M., Dixon, D.G., Le, X.C., 2014. Uptake and speciation of vanadium in the benthic invertebrate *Hyalella azteca*. Environ. Sci. Technol. 48, 731–738. https://doi.org/10.1021/es403252k.
Jeske, A., Gworek, B., 2012. Chromium, nickel and vanadium mobility in soils derived from fluvioglacial sands. J. Hazard Mater. 237–238, 315–322. https://doi.org/10.1016/j.jhazmat.2012.08.048.
Jiang, Y., Zhang, B., He, C., Shi, J., Borthwick, A.G.L., Huang, X., 2018. Synchronous vanadium(V) reduction and denitrification in groundwater using hydrogen as the sole electron donor. Water Res. 141, 289–296. https://doi.org/10.1016/j.watres.2018.05.033.
Johannesson, K.H., Lyons, W.B., Graham, E.Y., Welch, K.A., 2000. Oxyanion concentrations in eastern Sierra Nevada rivers - 3. Boron, molybdenum, vanadium, and tungsten. Aquat. Geochem. 6, 19–46. https://doi.org/10.1023/A:1009622219482.
Kabata-Pendias, A., 2001. Trace elements in soils and plants, third ed. CRC Press, Boca Raton, Florida, USA.
Kaplan, D.I., Adriano, D.C., Carlson, C.L., Sajwan, K.S., 1990a. Vanadium - toxicity and accumulation by beans. Water Air Soil Pollut. 49, 81–91. https://doi.org/10.1007/BF00279512.
Kaplan, D.I., Sajwan, K.S., Adriano, D.C., Gettier, S., 1990b. Phytoavailability and toxicity of beryllium and vanadium. Water Air Soil Pollut. 53, 203–212. https://doi.org/10.1007/BF00170737.
Kaur, N., Singh, B., Kennedy, B.J., Gräfe, M., 2009. The preparation and characterization of vanadium-substituted goethite: the importance of temperature. Geochim. Comsochim. Acta 73, 582–593. https://doi.org/10.1016/j.gca.2008.10.025.
Kelly, S., Hesterberg, D., Ravel, B., 2008. Analysis of soils and minerals using X-ray absorption spectroscopy. In: Ulery, D.L., Drees, R.L. (Eds.), Methods of soil analysis, Part 5, Mineralogical methods. SSSA Book Series, SSSA, Madison, WI, pp. 387–464 2008.
Kinniburgh, D.G., van Riemsdijk, W.H., Koopal, L.K., Borkovec, M., Benedetti, M.F., Avena, M.J., 1999. Ion binding to natural organic matter: competition, heterogeneity, stoichiometry and thermodynamic consistency. Colloid. Surface. A151, 147–166. https://doi.org/10.1016/S0927-7757(98)00637-2.
Krachler, M., Mohl, C., Emons, H., Shotyk, W., 2003. Atmospheric deposition of V, Cr and Ni since the late Glacial: effects of climatic cycles, human impacts, and comparison with crustal abundances. Environ. Sci. Technol. 37, 2658–2667. https://doi.org/10.1021/es0263083.
Kraepiel, A.M.L., Dere, A.L., Herndon, E.M., Brantley, S.L., 2015. Natural and anthropogenic processes contributing to metal enrichment in surface soils of central Pennsylvania. Biogeochemistry 123, 265–283. https://doi.org/10.1007/s10533-015-0068-5.
Krakowiak, J., Lundberg, D., Persson, I., 2012. A coordination chemistry study of hydrated and solvated cationic vanadium ions in oxidation states +III, +IV and +V in solution and solid state. Inorg. Chem. 51, 9598–9609. https://doi.org/10.1021/ic300202f.
Larson, J.W., 1995. Thermochemistry of vanadium(5+) in aqueous solutions. J. Chem. Eng. Data 40, 1276–1280. https://doi.org/10.1021/je00022a030.
Larsson, M.A., Baken, S., Gustafsson, J.P., Hadialhejazi, G., Smolders, E., 2013. Vanadium bioavailability and toxicity to soil microorganisms and plants. Environ. Toxicol. Chem. 32, 2266–2273. https://doi.org/10.1002/etc.2322.
Larsson, M.A., Baken, S., Smolders, E., Cubadda, F., Gustafsson, J.P., 2015a. Vanadium bioavailability in soils amended with blast furnace slag. J. Hazard Mater. 296, 158–165. https://doi.org/10.1016/j.jhazmat.2015.04.034.
Larsson, M.A., D'Amato, M., Cubadda, F., Raggi, A., Öborn, I., Kleja, D.B., Gustafsson, J.P., 2015b. Long-term fate and transformations of vanadium in a pine forest soil with added converter lime. Geoderma 259–260, 271–278. https://doi.org/10.1016/j.geoderma.2015.06.012.
Larsson, M.A., Hadialhejazi, G., Gustafsson, J.P., 2017a. Vanadium sorption by mineral soils: development of a predictive model. Chemosphere 168, 925–932. https://doi.org/10.1016/j.chemosphere.2016.10.117.
Larsson, M.A., Persson, I., Sjöstedt, C., Gustafsson, J.P., 2017b. Vanadate complexation to ferrihydrite: X-ray absorption spectroscopy and CD-MUSIC modelling. Environ. Chem. 14, 141–150. https://doi.org/10.1071/EN16174.
Leblanc, C., Colin, C., Cosse, A., Delage, L., La Barre, S., Morin, P., Fiévet, B., Voiseaux, C., Ambroise, Y., Verhaeghe, E., Amouroux, D., Donard, O., Tessier, E., Potin, P., 2006. Iodine transfers in the coastal marine environment: the key role of brown algae and of their vanadium-dependent haloperoxidases. Biochimie 88, 1773–1785. https://doi.org/10.1016/j.biochi.2006.09.001.
Leblanc, C., Vilter, H., Fournier, J.B., Delage, L., Potin, P., Rebuffet, E., Michel, G., Solari, P.L., Feiters, M.C., Czjzek, M., 2015. Vanadium haloperoxidases: from the discovery 30 years ago to X-ray crystallographic and V K-edge absorption spectroscopic studies. Coord. Chem. Rev. 301–302, 134–146. https://doi.org/10.1016/j.ccr.2015.02.013.
Leckie, J.O., Appleton, A.R., Ball, N.B., Hayes, K.F., Honeyman, B.D., 1984. Adsorptive removal of trace elements from fly-ash pond effluents onto iron oxyhydroxide. EPRI RP-910-1. Electric Power Research Institute, Palo Alto, CA, USA.
Lee, K., Nalewajko, C., Jack, T.R., 1979. Effects of vanadium on freshwater algae. In: Proceedings of the fifth annual aquatic toxicity workshop, Hamilton, Ontario, Nov 7-9, 1978, vol. 862. Fisheries and Marine Service Technical Report, pp. 297–310.
Lehoux, A.P., Lockwood, C.L., Mayes, W.M., Stewart, D.I., Mortimer, R.J.G., Gruiz, K., Burke, I.T., 2013. Gypsum addition to soils contaminated by red mud: implications for aluminium, arsenic, molybdenum and vanadium solubility. Environ. Geochem. Health 35, 643–656. https://doi.org/10.1007/s10653-013-9547-6.

Levina, A., McLeod, A.I., Lay, P.A., 2014. Vanadium speciation by XANES spectroscopy: a three-dimensional approach. Chem. Eur J. 20, 12056–12060. https://doi.org/10.1002/chem.201403993.
Lewan, M.D., 1984. Factors controlling the proportionality of vanadium to nickel in crude oils. Geochem. Cosmochim. Acta 48, 2231–2238. https://doi.org/10.1016/0016-7037(84)90219-9.
Li, L., Kim, S., Wang, W., Vijayakumar, M., Nie, Z., Chen, B., Zhang, J., Xia, G., Hu, J., Graff, G., Liu, J., Yang, Z., 2011. A stable vanadium redox-flow battery with high energy density for large-energy density for large-scale energy storage. Adv. Energy Mater. 1, 394–400. https://doi.org/10.1002/aenm.201100008.
Liang, C.N., Tabatabai, M.A., 1977. Effects of trace elements on nitrogen mineralization in soils. Environ. Pollut. 12, 141–147. https://doi.org/10.1016/0013-9327(77)90017-9.
Liang, C.N., Tabatabai, M.A., 1978. Effects of trace elements on nitrification in soils. J. Environ. Qual. 7, 291–293. https://doi.org/10.2134/jeq1978.00472425000700020028x.
Liu, H., Jiang, S.J., 2002. Determination of vanadium in water samples by reaction cell inductively coupled plasma quadrupole mass spectrometry. J. Anal. At. Spectrom 17, 556–559. https://doi.org/10.1039/B111577B.
López, L., Lo Mónaco, S., Galarraga, F., Lira, A., Cruz, C., 1995. V/Ni ratio in maltene and asphaltene fractions of crude oils from the west Venezuelan basin: correlation studies. Chem. Geol. 119, 255–262. https://doi.org/10.1016/0009-2541(94)00100-M.
Lu, X.Q., Johnson, W.D., Hook, J., 1998. Reaction of vanadate with aquatic humic substances: An ESR and V-51 NMR study. Environ. Sci. Technol. 32, 2257–2263. https://doi.org/10.1021/es970930r.
Lyalkova, N.N., Yurkova, N.A., 1992. Role of microorganisms in vanadium concentration and dispersion. Geomicrobiol. J. 10, 15–26. https://doi.org/10.1080/01490459209377901.
Mandiwana, K.L., Panichev, N., 2004. Electrothermal atomic absorption spectrophotometric determination of vanadium(V) in soil after leaching with Na_2CO_3. Anal. Chim. Acta 517, 201–206. https://doi.org/10.1016/j.aca.2004.04.068.
Martin, H.W., Kaplan, D.I., 1998. Temporal changes in cadmium, thallium, and vanadium mobility in soil and phytoavailability under field conditions. Water Air Soil Pollut. 101, 399–410. https://doi.org/10.1023/A:1004906313547.
Maylotte, D.H., Wong, J., St Peters, R.L., Lytle, F.W., Greegor, R.G., 1981. X-ray spectroscopic investigation of trace vanadium sites in coal. Science 214 (4520), 554–556. https://doi.org/10.1126/science.214.4520.554.
McCann, M., Wagner, M., Hasse, H., 2013. A thermodynamic model for vanadate in aqueous solution – equilibria and reaction enthalpies. J. Chem. Soc. Dalton Trans. 42, 2622–2628. https://doi.org/10.1039/c2dt31993d.
McCann, M., Imle, M., Hasse, H., 2015. Carbonate complexes of vanadate. Polyhedron 95, 81–85. https://doi.org/10.1016/j.poly.2015.03.004.
McCrindle, C.M.E., Mokantla, E., Duncan, N., 2001. Peracute vanadium toxicity in cattle grazing near a vanadium mine. J. Environ. Monit. 3, 580–582. https://doi.org/10.1039/B107244G.
McDonough, W.F., Sun, S., 1995. The composition of the Earth. Chem. Geol. 120, 223–253. https://doi.org/10.1016/0009-2541(94)00140-4.
Messerschmidt, A., Wever, R., 1995. X-ray structure of a vanadium-containing enzyme: chloroperoxidase from the fungus Curvilaria inaequalis. Proc. Nat. Acad. Sci. USA 93, 392–396. https://doi.org/10.1073/pnas.93.1.392.
Mikkonen, A., Tummavuori, J., 1994. Retention of vanadium(V) by three Finnish mineral soils. Eur. J. Soil Sci. 45, 361–368. https://doi.org/10.1111/j.1365-2389.1994.tb00520.x.
Mikkonen, H.G., van de Graaff, R., Collins, R.N., Dasika, R., Wallis, C.J., Howard, D.L., Reichman, S.M., 2019. Immobilisation of geogenic arsenic and vanadium in iron-rich sediments and iron stone deposits. Sci. Total Environ. 654, 1072–1083. https://doi.org/10.1016/j.scitotenv.2018.10.427.
Milne, C.J., Kinniburgh, D.G., van Riemsdijk, W.H., Tipping, E., 2003. Generic NICA-Donnan model parameters for metal-ion binding by humic substances. Environ. Sci. Technol. 37, 958–971. https://doi.org/10.1021/es0258879.
Minelli, L., Veschetti, E., Giammanco, S., Mancini, G., Ottaviani, M., 2000. Vanadium in Italian waters: monitoring and speciation of V(IV) and V(V). Microchem. J. 67, 83–90. https://doi.org/10.1016/S0026-265X(00)00102-8.
Mišik, M., Burke, I.T., Reismüller, M., Pichler, C., Rainer, B., Mišikova, K., Mayes, W.M., Knasmueller, S., 2014. Red mud a byproduct of aluminium production contains soluble vanadium that causes genotoxic and cytotoxic effects in higher plants. Sci. Total Environ. 493, 883–890. https://doi.org/10.1016/j.scitotenv.2014.06.052.
Monakhov, I.N., Khromov, S.V., Chernousov, P.I., Yusfin, Y.S., 2004. The flow of vanadium-bearing materials in industry. Metallurgist 48, 381–385. https://doi.org/10.1023/B:MELL.0000048420.68839.2a.
Naeem, A., Westerhoff, P., Mustafa, S., 2007. Vanadium removal by metal (hydr)oxide adsorbents. Water Res. 41, 1596–1602. https://doi.org/10.1016/j.watres.2007.01.002.
Nalewajko, C., Lee, K., Jack, T.R., 1995a. Effects of vanadium on freshwater phytoplankton photosynthesis. Water Air Soil Pollut. 81, 93–105. https://doi.org/10.1007/BF00477258.
Nalewajko, C., Lee, K., Olaveson, M., 1995b. Responses of freshwater algae to inhibitory vanadium concentrations: the role of phosphorus. J. Phycol. 31, 332–343. https://doi.org/10.1111/j.0022-3646.1995.00332.x.
Nedrich, S.M., Chappaz, A., Hudson, M.L., Brown, S.S., Burton jr., A., 2018. Biogeochemical controls on the speciation and aquatic toxicity of vanadium and other metals in sediments from a river reservoir. Sci. Total Environ. 612, 313–320. https://doi.org/10.1016/j.scitotenv.2017.08.141.
Nesbitt, J.A., Lindsay, M.B.J., 2017. Vanadium geochemistry of oil sands fluid petroleum coke. Environ. Sci. Technol. 51, 3102–3109. https://doi.org/10.1021/acs.est.6b05682.
Nesbitt, J.A., Lindsay, M.B.J., Chen, N., 2017. Geochemical characteristics of oil sands fluid petroleum coke. Appl. Geochem. 76, 148–158. https://doi.org/10.1016/j.apgeochem.2016.11.023.
Nielsen, S.G., Prytulak, J., Halliday, A.N., 2011. Determination of precise and accurate 51V/50V isotope ratios by MC-ICP-MS, part 1: chemical separation of vanadium and mass spectometric protocols. Geostand. Geoanal. Res. 35, 293–306. https://doi.org/10.1111/j.1751-908X.2011.00106.x.
Nielsen, S.G., Owens, J.D., Horner, T.J., 2016. Analysis of high-precision vanadium isotope ratios by medium resolution ICP-MS. J. Anal. At. Spectrom. 31, 531–536. https://doi.org/10.1039/C5JA00397K.
Nriagu, J.O., 1998. Vanadium in the environment: Part 1, Chemistry and biochemistry. Wiley.
Nuester, J., Vogt, S., Newville, M., Kustka, A.B., Twining, B.S., 2012. The unique biogeochemical signature of the marine diazotroph *Trichodesmium*. Front. Microbiol. 3, 150. https://doi.org/10.3389/fmicb.2012.00150.
Ona-Nguema, G., Morin, G., Juillot, F., Calas, G., Brown, G.E., 2005. EXAFS analysis of arsenite adsorption onto two-line ferrihydrite, hematite, goethite, and lepidocrocite. Environ. Sci. Technol. 39, 9147–9155. https://doi.org/10.1021/es050889p.
Ortiz-Bernad, I., Anderson, R.T., Vrionis, H.A., Lovley, D.R., 2004. Vanadium respiration by *Geobacter metallireducens:* novel strategy for in situ removal of vanadium from groundwater. Appl. Environ. Microbiol. 70, 3091–3095. https://doi.org/10.1128/AEM.70.5.3091-3095.2004.
Panichev, N., Mandiwana, K., Moema, D., Molatlhegi, R., Ngobeni, P., 2006. Distribution of vanadium(V) species between soil and plants in the vicinity of vanadium mine. J. Hazard Mater. 137, 649–653. https://doi.org/10.1016/j.jhazmat.2006.03.006.
Peacock, C.L., Sherman, D.M., 2004. Vanadium(V) adsorption onto goethite (α-FeOOH) at pH 1.5 to 12: A surface complexation model based on ab initio molecular geometries and EXAFS spectroscopy. Geochem. Cosmochim. Acta 68, 1723–1733. https://doi.org/10.1016/j.gca.2003.10.018.
Planchon, F.A.M., Boutron, C.F., Ferrari, C.P., Barbante, C., Cozzi, G., Cescon, P., Wolff, E.W., 2002. Changes in heavy metals in Antarctic snow from Coats land since the mid-19th to the late-20th century. Earth Planet. Sci. Lett. 200, 207–222. https://doi.org/10.1016/S0012-821X(02)00612-X.
Pokrovsky, O.S., Schott, J., 2002. Iron colloids/organic matter-associated transport of major and trace elements in small boreal rivers and their estuaries (NW Russia). Chem. Geol. 190, 141–179. https://doi.org/10.1016/S0009-2541(02)00115-8.
Poledniok, J., Buhl, F., 2003. Speciation of vanadium in soil. Talanta 59, 1–8. https://doi.org/10.1016/S0039-9140(02)00322-3.
Pourret, O., Dia, A., Gruau, G., Davranche, M., Bouhnik-Le Coz, M., 2012. Assessment of vanadium distribution in shallow groundwaters. Chem. Geol. 294–295, 89–102. https://doi.org/10.1016/j.chemgeo.2011.11.033.
Presslinger, H., Klepp, K.O., 2002. Vanadium in converter slags. Steel Res. 73, 522–525. https://doi.org/10.1002/srin.200200022.
Priest, C., Zhou, J., Jiang, D., 2017. Solvation of the vanadate ion in seawater conditions from molecular dynamics simulations. Inorg. Chim. Acta. 458, 39–44. https://doi.org/10.1016/j.ica.2016.12.027.
Prytulak, J., Nielsen, S.G., Halliday, A.N., 2011. Determination of precise and accurate 51V/50V isotope ratios by multi-collector ICP-MS, part 2: isotopic composition of six reference materials plus the Allende chondrite and verification tests. Geostand. Geoanal. Res. 35, 307–318. https://doi.org/10.1111/j.1751-908X.2011.00105.x.
Pyrzyńska, K., 2006. Selected problems in speciation analysis of vanadium in water samples. Chem. Anal. 51, 339–350 Warsaw.
Qian, Y., Gallagher, F.J., Feng, H., Wu, M., Zhu, Q., 2014. Vanadium uptake and translocation in dominant plant species on an urban coastal brownfield site. Sci. Total Environ. 476–477, 696–704. https://doi.org/10.1016/j.scitotenv.2014.01.049.
Rauret, G., López-Sanchez, J.F., Saquhillo, A., Rubio, R., Davidson, R., Ure, A., Quevauviller, P., 1999. Improvement of the BCR three-step extraction procedure prior to the certification of new sediment and soil reference materials. J. Environ. Monit. 1, 57–61. 1999. https://doi.org/10.1039/A807854H.
Ravel, B., Newville, M., 2005. Athena, Artemis, Haephestus: data analysis for X-ray absorption spectroscopy using IFEFFIT. J. Synchrotron Radiat. 12, 537–541. https://doi.org/10.1107/S0909049505012719.
Rees, J.A., Wandzilak, A., Maganas, D., Worster, N.I.C., Hugenbruch, S., Kowalska, J.K., Pollock, C.J., Lima, F.A., Finkelstein, K.D., DeBeer, S., 2016. Experimental and theoretical correlations between vanadium K-edge X-ray absorption and Kβ emission spectra. J. Biol. Inorg. Chem. 21, 793–805. https://doi.org/10.1007/s00775-016-1358-7.
Rees, J.A., Björnsson, R., Kowalska, J.K., Lima, F.A.,, Schlesier, J., Sippel, D., Weyhermüller, T., Einsle, O., Kovacs, J.A., DeBeer, S., 2017. Comparative electronic structures of nitrogenase FeMoco and FeVco. Dalton Trans. 46, 2445–2455. https://doi.org/10.1039/C7DT00128B.
Rehder, D., 2015. The role of vanadium in biology. Metallomics 7, 730–742. https://doi.org/10.1039/c4mt00304g.
Reijonen, I., Metzler, M., Hartikainen, H., 2016. Impact of soil pH and organic matter on the chemical bioavailability of vanadium species: the underlying basis for risk assessment. Environ. Pollut. 210, 371–379. https://doi.org/10.1016/j.envpol.2015.12.046.
Rietra, R.P.J.J., 2001. Relationship between the molecular structure and ion adsorption on goethite. PhD thesis. Wageningen University, Netherlands.
Rosborg, I., Nihlgård, B., Gerhardsson, L., Gernersson, M.L., Ohlin, R., Olsson, T., 2005. Concentrations of inorganic elements in bottled waters on the Swedish market. Environ. Geochem. Health 27, 217–227. https://doi.org/10.1007/s10653-004-1612-8.
Ruyters, S., Mertens, J., Vassilieva, E., Dehandschutter, B., Poffijn, A., Smolders, E., 2011. The red mud accident in Ajka (Hungary): plant toxicity and trace metal bioavailability in red mud contaminated soil. Environ. Sci. Technol. 45, 1616–1622. https://

doi.org/10.1021/es104000m.
Sahoo, S.K., 2015. Ediacaran ocean redox evolution. PhD Thesis. University of Nevada, Las Vegas, NV, USA.
Schiffer, S., Liber, K., 2017a. Toxicity of aqueous vanadium to zooplankton and phytoplankton species of relevance to the Athabasca oil sands region. Ecotoxicol. Environ. Saf. 137, 1–11. https://doi.org/10.1016/j.ecoenv.2016.10.040.
Schiffer, S., Liber, K., 2017b. Estimation of vanadium water quality benchmarks for the protection of aquatic life with relevance to the Athabasca oil sands region using species sensitivity distributions. Environ. Toxicol. Chem. 36, 3034–3044. https://doi.org/10.1002/etc.3871.
Schlesinger, W.H., Klein, E.M., Vengosh, A., 2017. Global biogeochemical cycle of vanadium. Proc. Natl. Acad. Sci. Unit. States Am. 114, E11092–E11100. https://doi.org/10.1073/pnas.1715500114.
Schuth, S., Horn, I., Brüske, A., Wolff, P.E., Weyer, S., 2017. First vanadium isotope analyses of V-rich minerals by femtosecond laser ablation and solution nebulization MC-ICP-MS. Ore Geol. Rev. 81, 1271–2186. https://doi.org/10.1016/j.oregeorev.2016.09.028.
Schwertmann, U., Pfab, G., 1994. Structural vanadium in synthetic goethite. Geochem. Cosmochim. Acta 58, 4349–4352. https://doi.org/10.1016/0016-7037(94)90338-7.
Schwertmann, U., Pfab, G., 1996. Structural vanadium and chromium in lateritic iron oxides: genetic implications. Geochem. Cosmochim. Acta 60, 4279–4283. https://doi.org/10.1016/S0016-7037(96)00259-1.
Scott, C., Slack, J.F., Kelley, K.D., 2017. The hyper-enrichment of V and Zn in black shales of the Late Devonian-Early Mississippian Bakken formation (USA). Chem. Geol. 452, 24–33. https://doi.org/10.1016/j.chemgeo.2017.01.026.
Seargeant, L.E., Stinson, R.A., 1979. Inhibition of human alkaline phosphatases by vanadate. Biochem. J. 181, 247–250. https://doi.org/10.1042/bj1810247.
Shacklette, H.T., Boerngen, J.G., 1984. Element concentrations in soils and other surficial materials of the conterminous United States. US Government Printing Office, Washington DC, USA USGS Professional Paper 1270.
Shafer, M.M., Toner, B.M., Overdier, J.T., Schauer, J.J., Fakra, S.C., Hu, S., Herner, J.D., Ayala, A., 2012. Chemical speciation of vanadium in particulate matter emitted from diesel vehicles and urban atmospheric aerosols. Environ. Sci. Technol. 46, 189–195. https://doi.org/10.1021/es200463c.
Shaheen, S.M., Rinklebe, J., 2018. Vanadium in thirteen different soil profiles originating from Germany and Egypt: geochemical fractionation and potential mobilization. Appl. Geochem. 88B, 288–301. https://doi.org/10.1016/j.apgeochem.2017.02.010.
Shaheen, S.M., Rinklebe, J., Frohne, T., White, J.R., DeLaune, R.D., 2014. Biogeochemical factors governing cobalt, nickel, selenium, and vanadium dynamics in periodically flooded Egyptian North Nile delta rice soils. Soil Sci. Soc. Am. J. 78, 1065–1078. https://doi.org/10.2136/sssaj2013.10.0441.
Shi, Y.X., Mangal, V., Guéguen, C., 2016. Influence of dissolved organic matter on dissolved vanadium speciation in the Churchill River estuary (Manitoba, Canada). https://doi.org/10.1016/j.chemosphere.2016.03.124.
Shieh, C.S., Duedall, I.W., 1988. Role of amorphous ferric oxyhydroxide in removal of anthropogenic vanadium from seawater. Mar. Chem. 25, 121–139. https://doi.org/10.1016/0304-4203(88)90060-6.
Shiller, A.M., Mao, L., 1999. Dissolved vanadium on the Louisiana Shelf: effect of oxygen depletion. Cont. Shelf Res. 19, 1007–1020. https://doi.org/10.1016/S0278-4343(99)00005-9.
Shiller, A.M., Mao, L., 2000. Dissolved vanadium in rivers: effect of silicate weathering. Chem. Geol. 165, 13–22. https://doi.org/10.1016/S0009-2541(99)00160-6.
Sippel, D., Einsle, O., 2017. The structure of vanadium nitrogenase reveals an unusual bridging ligand. Nat. Chem. Biol. 13, 956–960. https://doi.org/10.1038/nchembio.2428.
Smit, C.E., 2012. Environmental risk limits for vanadium in water. A proposal for water quality standards in accordance with the Water Framework Directive. RIVM Letter Report 601714021/2012. National Institute for Public Health and the Environment 2012.
Smith, R.M., Martell, A.E., Motekaitis, R.J., 2004. NIST critically selected stability constants of metal complexes database. NIST, Gaithersburg, MD, USA NIST standard reference database 46, version 8.0.
Smith, P.G., Boutin, C., Knopper, L., 2013. Vanadium pentoxide phytotoxicity: effects of species selection and nutrient concentration. Arch. Environ. Contam. Toxicol. 64, 87–96. https://doi.org/10.1007/s00244-012-9806-z.
Smolders, E., Oorts, K., van Sprang, P., Schoeters, I., Janssen, C.R., McGrath, S.P., McLaughlin, M.J., 2009. Toxicity of trace metals in soil as influenced by soil type and aging after contamination: using calibrated bioavailability models to set ecological soil standards. Environ. Toxicol. Chem. 28, 1633–1642. https://doi.org/10.1897/08-592.1.
Stolpe, B., Hassellöv, M., Andersson, K., Turner, D.R., 2005. High resolution ICPMS as an on-line detector for flow field-flow fractionation; multi-element determination of colloidal size distributions in a natural water sample. Anal. Chim. Acta 535, 109–121. https://doi.org/10.1016/j.aca.2004.11.067.
Sun, W., Xiao, E., Krumins, V., Häggblom, M.M., Dong, Y., Pu, Z., Li, B., Wang, Q., Xiao, T., Li, F., 2018. Rhizosphere microbial response to multiple metal(loid)s in different contaminated arable soils indicates crop-specific metal-microbe interactions. Appl. Environ. Microbiol. 84, e00701–e00718. https://doi.org/10.1128/AEM.00701-18.
Sutton, S.R., Kamer, J., Papike, J., Delaney, J.S., Shearer, C., Newville, M., Eng, P., Rivers, M., Dyar, M.D., 2005. Vanadium K edge XANES of synthetic and natural basaltic glasses and application to microscale oxygen barometry. Geochem. Cosmochim. Acta 69, 2333–2348. https://doi.org/10.1016/j.gca.2004.10.013.
Szalay, A., Szilagyi, M., 1967. The association of vanadium with humic acids. Geochem. Cosmochim. Acta 31, 1–6. https://doi.org/10.1016/0016-7037(67)90093-2.
Telfeyan, K., Johannesson, K.H., Mohajerin, T.J., Palmore, C.D., 2015. Vanadium geochemistry along groundwater flow paths in contrasting aquifers of the United States: Carrizo Sand (Texas) and Oasis Valley (Nevada) aquifers. Chem. Geol. 410, 63–78. https://doi.org/10.1016/j.chemgeo.2015.05.024.
Telfeyan, K., Breaux, A., Kim, J., Kolker, A.S., Cable, J.E., Johannesson, K.H., 2018. Cycling of oxyanion-forming trace elements in groundwaters from a freshwater deltaic marsh. Estuar. Coast Shelf Sci. 204, 236–263. https://doi.org/10.1016/j.ecss.2018.02.024.
Templeton, G.D., Chasteen, N.D., 1980. Vanadium-fulvic acid chemistry: conformational and binding studies by electron spin probe techniques. Geochem. Cosmochim. Acta 44, 741–752. https://doi.org/10.1016/0016-7037(80)90163-5.
Terzano, R., Spagnuolo, M., Vekemans, B., De Nolf, W., Janssens, K., Falkenberg, G., Fiore, S., Ruggiero, P., 2007. Assessing the origin and fate of Cr, Ni, Cu, Zn, Pb, and V in industrial polluted soil by combined microspectroscopic techniques and bulk extraction methods. Environ. Sci. Technol. 41, 6762–6769. https://doi.org/10.1021/es070260h.
Tessier, A., Campbell, P.G.C., Bisson, M., 1979. Sequential extraction procedure for the speciation of particulate trace metals. Anal. Chem. 51, 844–851. https://doi.org/10.1021/ac50043a017.
Thompson, A., Attwood, D., Gullikson, E., Howells, M., Kim, K.-J., Kirz, J., Kortright, J., Lindau, I., Pianetta, P., Robinson, A., Scofield, J., Underwood, J., Williams, G., Winck, H., 2009. X-ray Data Booklet. Lawrence Berkeley National Laboratory, University of California, Berkeley, CA, USA.
Tian, L., Yang, J., Alewell, C., Huang, J.H., 2014. Speciation of vanadium in Chinese cabbage (*Brassica rapa* L.) and soils in response to different levels of vanadium in soils and cabbage growth. Chemosphere 111, 89–95. https://doi.org/10.1016/j.chemosphere.2014.03.051.
Tian, L., Yang, J., Huang, J.H., 2015. Uptake and speciation of vanadium in the rhizosphere soils of rape (*Brassica juncea* L.). Environ. Sci. Pollut. Res. 22, 9215–9223. https://doi.org/10.1007/s11356-014-4031-0.
Tiberg, C., Sjöstedt, C., Persson, I., Gustafsson, J.P., 2013. Phosphate effects on copper(II) and lead(II) sorption to ferrihydrite. Geochem. Cosmochim. Acta 120, 140–157. https://doi.org/10.1016/j.gca.2013.06.012.
Tipping, E., 1998. Humic ion-binding model VI: an improved description of the interactions of protons and metal ions with humic substances. Aquat. Geochem. 4, 3–48. https://doi.org/10.1023/A:1009627214459.
Tipping, E., Lofts, S., Sonke, J.E., 2011. Humic ion-binding model VII: a revised parameterisation of cation-binding by humic substances. Environ. Chem. 8, 225–235. https://doi.org/10.1071/EN11016.
Tribovillard, N., Algeo, T.J., Lyons, T., Riboulleau, A., 2006. Trace metals as paleoredox and paleoproductivity proxies: an update. Chem. Geol. 232, 12–32. https://doi.org/10.1016/j.chemgeo.2006.02.012.
Tyler, G., 1976. Influence of vanadium on soil phosphatase activity. J. Environ. Qual. 5, 216–217. https://doi.org/10.2134/jeq1976.00472425000500020023x.
van Zomeren, A., van der Laan, S.R., Kobesen, H.B.A., Huijgen, W.J.J., Comans, R.N.J., 2011. Changes in mineralogical and leaching properties of converter steel slag resulting from accelerated carbonation at low CO_2 pressure. Waste Manag. 31 2246-2244. https://doi.org/10.1016/j.wasman.2011.05.022.
Ventura, G.T., Gall, L., Siebert, C., Prytulak, J., Szatmari, P., Hürlimann, M., Halliday, A.M., 2015. The stable isotope composition of vanadium, nickel, and molybdenum in crude oils. Appl. Geochem. 59, 104–117. https://doi.org/10.1016/j.apgeochem.2015.04.009.
Vitousek, P., Cassman, K., Cleveland, C., Crews, T., Field, C.B., Grimm, N.B., Howarth, R.W., Marino, R., Martinelli, R., Rastetter, E.B., Sprent, J.I., 2002. Towards an ecological understanding of nitrogen fixation. In: Boyer, E.W., Howarth, R.W. (Eds.), The nitrogen cycle at regional to global scales. Springer, Dordrecht. https://doi.org/10.1007/978-94-017-3405-9_1.
Wällstedt, T., Björkvald, L., Gustafsson, J.P., 2010. Increasing concentrations of arsenic and vanadium in (southern) Swedish streams. Appl. Geochem. 25, 1162–1175. https://doi.org/10.1016/j.apgeochem.2010.05.002.
Wang, J.F., Liu, Z., 1999. Effect of vanadium on the growth of soybean seedlings. Plant Soil 216, 47–51. https://doi.org/10.1023/A:1004723509113.
Wang, D., Sañudo Wilhelmy, S.A., 2009. Vanadium speciation and cycling in coastal waters. Mar. Chem. 117, 52–58. https://doi.org/10.1016/j.marchem.2009.06.001.
Wanty, R.B., Goldhaber, M.B., 1992. Thermodynamics and kinetics of reactions involving vanadium in natural systems: Accumulation of vanadium in sedimentary rocks. Geochem. Cosmochim. Acta 56, 1471–1483. https://doi.org/10.1016/0016-7037(92)90217-7.
Watt, J.A.J., Burke, I.T., Edwards, R.A., Malcolm, H.M., Mayes, W.M., Olszewska, J.P., Pan, G., Graham, M.C., Heal, K.V., Rose, N.L., Turner, S.D., Spears, B.M., 2018. Vanadium: a re-emerging environmental hazard. Environ. Sci. Technol (in press). https://doi.org/10.1021/acs.est.8b05560.
Wehrli, B., Stumm, W., 1989. Vanadyl in natural waters: adsorption and hydrolysis promote oxygenation. Geochem. Cosmochim. Acta 53, 69–77. https://doi.org/10.1016/0016-7037(89)90273-1.
Wenzel, W.W., Kirchbaumer, N., Prohaska, T., Stingeder, G., Lombi, E., Adriano, D.C., 2001. Arsenic fractionation in soils using an improved sequential extraction procedure. Anal. Chim. Acta 436, 309–323. https://doi.org/10.1016/S0003-2670(01)00924-2.
Whitfield, M., Turner, D.R., 1978. Water-rock partition coefficients and the composition of seawater and river water. Nature 278, 132–137. https://doi.org/10.1038/278132a0.
Wilke, B.M., 1989. Long-term effects of different pollutants on nitrogen transformations in a sandy cambisol. Biol. Fertil. Soils 7, 254–258. https://doi.org/10.1007/BF00709657.
Wisawapipat, W., Kretzschmar, R., 2017. Solid-phase speciation and solubility of vanadium in highly weathered soils. Environ. Sci. Technol. 51, 8254–8262. https://doi.org/10.1021/acs.est.7b01005.

Wong, J., Lytle, F.W., Messmer, R.P., Maylotte, D.H., 1984. K-edge absorption spectra of selected vanadium compounds. Phys. Rev. B30, 5596–5610. https://doi.org/10.1103/PhysRevB.30.5596.

Wright, M.T., Belitz, K., 2010. Factors controlling the regional distribution of vanadium in groundwater. Gr. Water 48, 515–525. https://doi.org/10.1111/j.1745-6584.2009.00666.x.

Wright, M.T., Stollenwerk, K.G., Belitz, K., 2014. Assessing the solubility controls on vanadium in groundwater, northeastern San Joaquin Valley, CA. Appl. Geochem. 48, 41–52. https://doi.org/10.1016/j.apgeochem.2014.06.025.

Wu, F., Qin, T., Li, X., Liu, Y., Huang, J.-H., Wu, Z., Huang, F., 2015. First-principles investigation of vanadium isotope fractionation in solution and during adsorption. Earth Planet. Sci. Lett. 426, 216–224. https://doi.org/10.1016/j.epsl.2015.06.048.

Wu, F., Qi, Y., Yu, H., Tian, S., Hou, Z., Huang, F., 2016. Vanadium isotope measurement by MC-ICP-MS. Chem. Geol. 421, 17–25.

Wu, F., Owens, J.D., Huang, T., Sarafian, A., Huang, K.F., Sen, I.S., Horner, T.J., Blusztajn, J., Morton, P., Nielsen, S.G., 2018. Vanadium isotope composition of seawater. Geochem. Cosmochim. Acta (in press). https://doi.org/10.1016/j.gca.2018.10.010.

Xiao, X., Yang, M., Guo, Z., Jiang, Z., Liu, Y., Cao, X., 2015. Soil vanadium pollution and microbial response characteristics from stone coal smelting district. Trans. Nonferrous Metals Soc. China 25, 1271–1278. https://doi.org/10.1016/S1003-6326(15)63727-X.

Xiao, X., Jiang, Z., Guo, Z., Wang, M., Zhu, H., Han, X., 2017. Effect of simulated acid rain on leaching and transformation of vanadium in paddy soils from stone coal smelting area. Process Saf. Environ. Protect. 109, 697–703. https://doi.org/10.1016/j.psep.2017.05.006.

Yang, J., Huang, J.-H., Lazzarro, A., Tang, Y., Zeyer, J., 2014. Response of soil enzyme activity and microbial community in vanadium-loaded soil. Water Air Soil Pollut. 225, 2012. https://doi.org/10.1007/s11270-014-2012-z.

Yin, H., Feng, X., Tan, W., Koopal, L.K., Hu, T., Zhu, M., Liu, F., 2015. Structure and properties of vanadium(V)-doped hexagonal turbostratic birnessite and its enhanced scavenging of Pb^{2+} from solutions. J. Hazard Mater. 288, 80–88. https://doi.org/10.1016/j.jhazmat.2015.01.068.

Zhang, Y., Moore, J.N., 1994. Selenium fractionation and speciation in a wetland system. Environ. Sci. Technol. 30, 2613–2619. https://doi.org/10.1021/es960046l.

Zhang, B., Hao, L., Tian, C., Yuan, S., Feng, C., Ni, J., Borthwick, A.G.L., 2015. Microbial reduction and precipitation of vanadium (V) in groundwater by immobilized mixed anaerobic culture. Bioresour. Technol. 192, 410–417. https://doi.org/10.1016/j.biortech.2015.05.102.

Zhang, B., Qiu, R., Lu, L., Chen, X., He, C., Lu, J., Ren, Z.J., 2018a. Autotrophic vanadium (V) bio-reduction in groundwater by elemental sulfur and zerovalent iron. Environ. Sci. Technol. 52, 7434–7442. https://doi.org/10.1021/acs.est.8b01317.

Zhang, W., Jiang, J., Li, K., Li, T., Li, D., Wang, J., 2018b. Amendment of vanadium-contaminated soil with soil conditioners: a study based on pot experiments with canola plants (*Brassica campestris* L.). Int. J. Phytoremediation 20, 454–461. https://doi.org/10.1080/15226514.2017.1365345.

Žižić, M., Ducic, T., Grolimund, D., Bajuk-Bogdanović, D., Nikolić, M., Stanić, M., Krizak, S., Zakrzewska, J., 2015. X-ray absorption near-edge structure micro-spectroscopy study of vanadium speciation in *Phycomyces blakesleeanus* mycelium. Anal. Bioanal. Chem. 407, 7487–7496. https://doi.org/10.1007/s00216-015-8916-7.

Žižić, M., Miladinović, Z., Stanić, M., Hadžibrahimović, M., Živić, M., Zakrzewska, J., 2016. ^{51}V NMR investigation of cell-associated vanadate species in *Phycomyces blakesleeanus* mycelium. Res. Microbiol. 167, 521–528. https://doi.org/10.1016/j.resmic.2016.04.012.